Viscoelastic Modeling of Extrusion Film Casting for Polymer Melts: Investigation of Flow Stability

Ing. Tomáš Barbořík, Ph.D.

Doctoral Thesis Summary

Tomas Bata University in Zlín

Tomas Bata University in Zlín
Faculty of Technology

Doctoral Thesis Summary

Viscoelastic Modeling of Extrusion Film Casting for Polymer Melts: Investigation of Flow Stability

Viskoelastické modelování extruzního lití polymerních tavenin na válec: Výzkum stability toku

Author:	**Ing. Tomáš Barbořík, Ph.D.**
Degree programme:	P2808 Chemistry and Materials Technology
Degree course:	2808V006 Technology of Macromolecular Compounds
Supervisor:	prof. Ing. Martin Zatloukal, Ph.D., DSc.
Reviewers:	prof. Ing. Kamil Wichterle, DrSc., dr. h. c. prof. Ing. Karel Kolomazník, DrSc. doc. RNDr. Jiří Vlček, CSc.

Zlín, December 2018

© Tomáš Barbořík

Published by **Tomas Bata University in Zlín** in the Edition **Doctoral Thesis Summary.**
The publication was issued in the year 2018.

Key words in Czech: *Extruzní lití na válec, Neck-in defekt („krčkování“), Viskoelastické modelování, Numerická analýza, Polymer, Jednoosá, tahová viskozita, Planární tahová viskozita, Zatvrzování, Teplotou a tokem indukovaná krystalizace, Koeficient přestupu tepla, Konstituční rovnice, Modifikovaný Leonovův model*

Key words: *Extrusion film casting, Neck-in phenomenon, Viscoelastic modelling, Numerical analysis, Polymer, Extensional uniaxial viscosity, Extensional planar viscosity, Strain hardening, Temperature and stress induced crystallization, Heat transfer coefficient, Constitutive equations, Modified Leonov model*

Full text of the scientific publication is available in the Library of TBU in Zlín.

ISBN 978-80-7454-818-5

ACKNOWLEDGEMENT

At this place, I would like to express my deepest thanks to my supervisor, Prof. Martin Zatloukal for his ideas, encouragement, guidance, patient, kind words and a great deal of time that he spent with me on getting over the small hurdles that occasionally appeared during a course of my study.

I would also like to thank Prof. Costas Tzoganakis for made it possible to spend my Canada research stay in such a vibrant environment as University of Waterloo without doubts is, for his kind advice and valuable comments on my research topic. This stay could not have been accomplished without the financial support provided by Tomas Bata University and Faculty of Technology and is also greatly appreciated.

I also wish to acknowledge Grant Agency of the Czech Republic (Grant registration No. 16-05886S) for the financial support.

Furthermore, I would especially like to thank my colleague and friend Jiri Drabek for being a companion over those great years spent at the university.

Last but not least, I wish to thank all my family for their persisting support and encouragement toward me at all times.

ABSTRACT

In the first part of this Ph.D. Thesis, the extrusion film casting process has been presented and negative phenomena that represent serious process limitation have been discussed. Following section is dedicated to the listing of both experimental and theoretical works and different mathematical models describing the extensional kinematic in film casting that have been published since 1970s. In the next section, novel viscoelastic extrusion film casting model utilizing 1.5D membrane approximation was derived considering single-mode modified Leonov model as the viscoelastic constitutive equation, energy equation, constant heat transfer coefficient, advanced crystallization kinetics taking into account the role of temperature, cooling rate and molecular stretch, crystalline phase dependent modulus and temperature dependent relaxation time. The model has been successfully validated for branched low-density polyethylenes and linear isotactic polypropylenes by using suitable experimental data taken from the open literature. The model has consequently been used for systematic parametric study in order to reveal the role of variety dimensionless variables (such as planar to uniaxial extensional viscosity ratio, extensional strain hardening, Deborah number, second to first normal stress difference ratio at the die exit, draw ratio, heat transfer coefficient and flow induced crystallization) on polymer melt/solid behavior during the extrusion film casting process with specific attention to unwanted neck-in phenomenon. Obtained knowledge together with the suggested model can be used for optimization of the extrusion die design (influencing flow history and thus die exit stress state), molecular architecture of polymer melts, processing conditions in order to minimize neck-in phenomenon as well as to optimize the production of flat polymeric films and porous membranes via extrusion film casting technology.

ABSTRAKT

Úvodní část této disertační práce je věnována popisu výroby tenkých polymerních filmů pomocí technologie lití na válec a souvisejících nestabilit toku, které mohou, pokud nastanou, redukovat procesní okno, a tak významným způsobem přispět k omezení produktivity a efektivity této technologie. V navazující části je podán přehled prací věnovaných této problematice jak z hlediska experimentálního, tak teoretického se zvláštním zřetelem na matematické modely popisující kinematiku daného procesu, které svým vznikem sahají až do 70. let minulého století. V další části práce je odvozen nový viskoelastický model pro technologii extruzního lití na válec, který je založen na 1.5D membránové aproximaci, konstituční rovnici modifikovaného Leonovova modelu, rovnici energie uvažující konstantní součinitel přestupu tepla, pokročilé kinetice krystalizace zohledňující vliv teploty, rychlosti chlazení a intenzity protažení makromolekulárních řetězců, dále na krystalinitě závislém modulu a teplotně závislém relaxačním čase. Model byl úspěšně validován pro rozvětvené nízkohustotní polyethyleny a lineární izotaktické polypropyleny za použití vhodných experimentálních dat převzatých z dostupné literatury. Následně byla provedena systematická parametrická analýza s cílem odhalit vliv materiálových a procesních parametrů vyjádřených pomocí řady, převážně bezrozměrných proměnných (jako např. poměru planární a jednoosé tahové viskozity, stupně zatvrzení při jednoosém protahování, Debořina čísla, poměru druhého a prvního rozdílu normálových napětí na konci vytlačovací hlavy, dloužícího poměru, koeficientu přestupu tepla nebo molekulárního protažení vedoucího k tokem indukované krystalizaci) na chování polymerní taveniny při procesu odlévání vytlačovaného filmu na válec se zvláštní pozorností k nežádoucímu jevu neck-in. Získané poznatky společně s nově navrženým modelem je možné využít k optimalizaci designu vytlačovacích hlav (ovlivňující tokovou historii a napětí na konci výstupní štěrbiny), molekulární architektury polymerních řetězců a zpracovatelských podmínek, a to jak za účelem minimalizace nestabilit typu neck-in, tak k optimalizaci výroby plochých polymerních fólií a polopropustných membrán pomocí technologie extruzního lití na válec.

LIST OF PAPERS

The following papers are encompassed in this doctoral thesis.

PAPER I

On the Role of Extensional Rheology and Deborah Number on the Neck-in Phenomenon During Flat Film Casting

Tomas Barborik, Martin Zatloukal and Costas Tzoganakis

International Journal of Heat and Mass Transfer. 2017. Vol. 111, p. 1296–1313.

AIS=0.767 and IF=3.891 by 2017.

PAPER II

Effect of die exit stress state, Deborah number, uniaxial and planar extensional rheology on the neck-in phenomenon in polymeric flat film production

Tomas Barborik and Martin Zatloukal

Journal of Non-Newtonian Fluid Mechanics. 2018. Vol. 255, p. 39–56.

AIS=0.769 and IF=2.293 by 2017.

PAPER III

Effect of heat transfer coefficient, draw ratio and die exit temperature on the production of flat iPP membranes

Tomas Barborik and Martin Zatloukal

Submitted for publication in International Journal of Heat and Mass Transfer.

PAPER IV

Viscoelastic simulation of extrusion film casting for linear iPP including stress induced crystallization

Tomas Barborik and Martin Zatloukal

Considered for publication in Journal of Rheology.

CONTENTS

ACKNOWLEDGEMENT 3
ABSTRACT 4
ABSTRAKT 5
LIST OF PAPERS 6
CONTENTS 8
STATE OF THE EXTRUSION FILM CASTING PROCESS 10
1. The Film Casting Process 10
1.1 Process Description 10
1.2 Flow Instabilities 12
1.2.1 Neck-in 13
1.2.2 Edge-beading 14
1.2.3 Draw Resonance 15
2. Mathematical Modeling of the Extrusion Film Casting Process 17
2.1 Literature Review 17
2.2 Mathematical models 22
2.2.1 One-dimensional Film Casting Model of Infinite Width 23
2.2.2 One-dimensional Film Casting Model of Varying Width 24
2.2.3 Two-dimensional Film Casting Model 24
THE AIMS OF THE DOCTORAL RESEARCH WORK 26
3. Viscoelastic Modeling of Non-isothermal Extrusion Film Casting Process Considering Temperature and Stress Induced Crystallization 27
3.1 Modified Leonov Model 27
3.2 Membrane Model of Film Casting 28
3.2.1 Velocity Field 29
3.2.2 Continuity Equation 30
3.2.3 Momentum Conservation Equation 31
3.2.4 The Stress-free Surface Boundary Condition 32
3.2.5 The Kinematic Free-surface Boundary Condition 32
3.2.6 Dimensionless Transformation 33

3.2.7 Extrusion Film Casting Model for the Modified Leonov Model ... 35
3.2.8 Energy Equation ... 37
3.2.9 Boundary Conditions ... 40
3.3 Numerical Scheme ... 41
SUMARIZATION OF THE RESEARCH PAPERS ... 44
THE THESIS CONTRIBUTION TO SCIENCE AND PRACTICE ... 51
CONCLUSION ... 52
REFERENCES ... 54
LIST OF FIGURES ... 63
LIST OF TABLES ... 64
LIST OF SYMBOLS ... 65
LIST OF PUBLICATIONS ... 73
CURRICULUM VITAE ... 77

STATE OF THE EXTRUSION FILM CASTING PROCESS

Extrusion film casting is an industrially significant process that has firm place among polymer processing technologies in practice. It can be categorized as a continuous, high-speed manufacturing process during that a thin, highly oriented films are produced. A great range of the plastic films and sheets produced by this technology can found their use in many different applications of daily and technical use: plastic bags, packing for consumer products, magnetic tapes for storage of audio video content, optical membranes for liquid crystal displays, air and vapor barriers, foils for capacitors, separator films for batteries in mobile devices and electric vehicles or as product for further processing by other technologies, such as thermoforming and biaxial orientation [1, 2].

Growing demands in an amount of production and quality of fabricated films together with introduction of new materials ask for new approaches in production line. Of particular interest and along the mechanical properties of the produced films is to keep film thickness uniform and width as close as possible to the designed extrusion die width. Besides, course of action based on a trial-and-error approach involved in design of film casting lines, the computer modeling can be utilized bringing the advantages of a reduced consumption of material during testing stage in commissioning of new casting line, a reduced time required for design and finally more efficient design. Thus, this strategy can provide better insight into the problem, extend the knowledge on relationships between process rheological quantities and suggest the possible approaches how to deal with them to optimize the process or give better understanding of underlying mechanics [2].

1. The Film Casting Process

1.1 Process Description

The production of film by the technology of extrusion film casting involves the several devices that take essential part in the entire process. The upstream part of the operation is processed by the extrusion machine where the polymer pellets are conveyed, homogenized and compressed by a screw, melted by means of dissipation and external heat sources, and thus the pressure require to push the polymer melt through the uniform slit die (center-fed T die or coat-hanger die) is generated. Once the polymer is emerged from the die that has typically small opening of about 1–2 mm, the second, downstream, stretching stage takes place where this thick sheet is intensively stretched in the machine direction by a constant rotating take-up drum, whose linear velocity is higher than the exit polymer velocity at the die, and simultaneously providing the sufficient cooling

rate to fix the final dimensions of so-called primary film, see Fig. 1. Moreover, by pulling the polymer melt at these conditions across the take-up length, the macromolecular orientation and thickness reduction to film is imposed. This solidified secondary film is subsequently handled by system of drums for winding-up by a winder to the rolls.

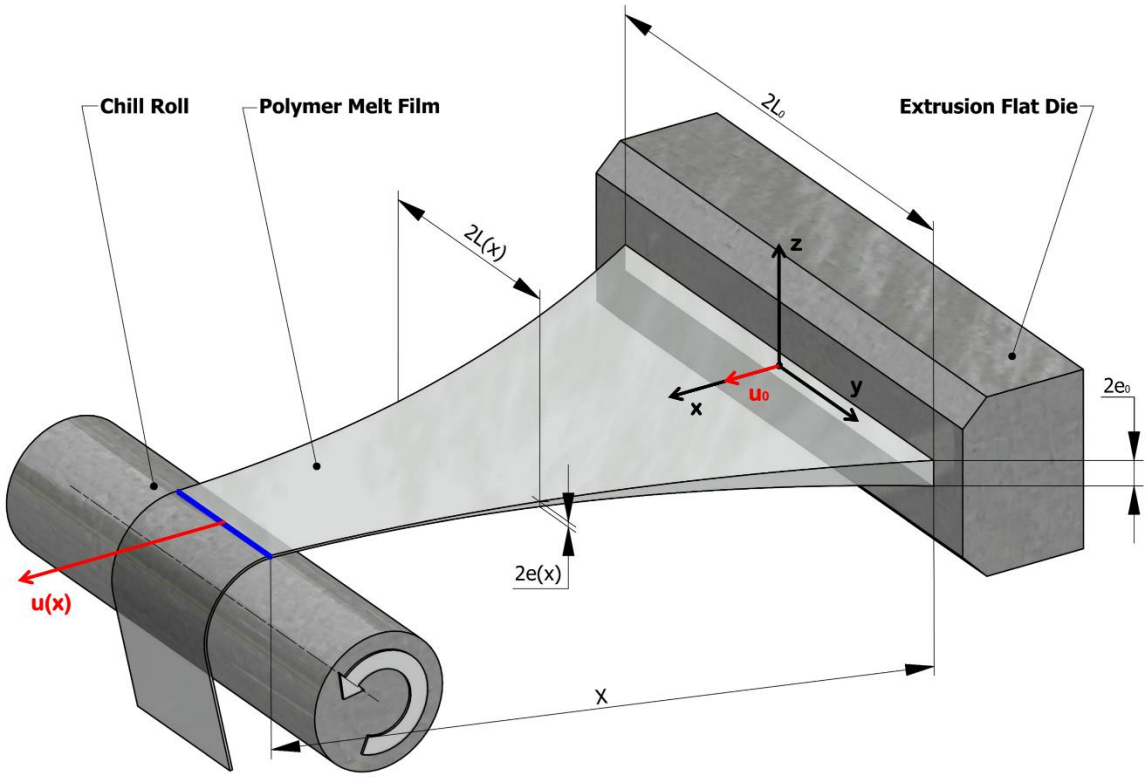

Fig. 1: Schematics of the extrusion film casting kinematics.

At the chill roll, several additional technological devices can be used to ensure a better contact line between film and a chill roll and to increase the rate of thermal transfer, such as air knife (a slit nozzle blows a jet of cooled air onto the film) or electrostatic pinning. In this composition, a high voltage wire is placed parallel to the grounded chill roll that creates an electrostatic discharged exerting the electrostatic force onto film to tight the contact film-chill roll. Another option with the similar result that can be used is vacuum box which function is based on suction of the air between the film and the chill roll and thus provide the negative pressure in this section for a better contact. Aside from cooling down on the chill roll, polymer film is naturally quenched, to a certain level depending also on the length of the drawing zone, by its travelling through the surrounding environment. This can be enhanced by introduction of convected air or an inert gas source to this section or by a film passage through a fluid bath [3]. Additionally, secondary film is about to undergo a treatment (plasma treating, heating and biaxial orientation) depending on the desired properties and purpose of the final product.

Specific attention should be paid to the polymer behavior in the drawing zone and to extensional conditions since this stage mainly determines the mechanical and optical properties that are accommodated by end-product [2, 4].

To produce highly functional films with tailored properties, multiple layers of different polymer melts can be coextruded and stretched, i.e. final properties of such film are constituted by traits of each layer. In this way, multilayer films with enhanced properties, such as impermeability to oxygen and moisture, strength, chemical resistance or color can be produced [5].

An alternative continuous manufacturing technology for the film production is called extrusion film blowing process. In this process, the extruded tube is inflated by an internal pressure into the shape of bubble having a thin wall thickness, quenched and hauled off. On par to this competing film production technology, films that are fabricated by extrusion film casting have a good transparency, thickness uniformity, smoother surface and are produced at higher production rate [2].

According to the current industrial practice where the wide variety of films is manufactured with requirement on its use in heterogeneous application, a broad range of materials is processed by producers for film casting technology. Frequently used polymeric materials include low density polyethylene, LDPE; high density polyethylene, HDPE; linear low density polyethylene, LLDPE; polypropylene, PP; polyethylene terephthalate, PET; and polystyrene, PS. Extrusion film casting is suitable for low viscosity polymers as well [6].

Owning to vast application variety of these films, there is request for production of wide range of sizes. Film width can range from 0.1 m to 10 m, thickness from 20 μm to 2000 μm [4] at production rate that varies from 70 to 200 m/min. The variation in thickness is reported ranging from 3 to 5 % [1].

1.2 Flow Instabilities

Several polymer processes involve the situation in which the polymer is stretched after initial extrusion. The presence of an air-polymer interface in the drawing zone allows to develop different kinds flow instabilities that place a serious limitation on required film quality and quantity. Their formation is influenced by the processing conditions, heat transfer and rheology of processed polymer. Some of them are observed in most cases, such as neck-in and edge-beading and others only under certain conditions that make the process unstable, such as draw resonance and film rupture. In the following subsections, their description is provided.

1.2.1 Neck-in

Upon exiting the die, the extruded polymer in form of thick sheet exhibits swelling due to viscoelastic nature of the most of the polymers. This molecular stress relaxation is consequently influenced by velocity field rearrangement that takes place during a transition from a confined shear flow in slit die to the extensional one in downstream. As a polymer sheet is hauled off further downstream and stable processing conditions are satisfied, its cross-sectional dimensions are monotonically reduced due to external drawing force exerted on sheet by a rotating take-up drum. Aside from desirable reduction in the film thickness, the reduction in film width is experienced. This defect is called neck-in and can be defined as the difference between film half-width at the die exit and final half-width of solidified film (Fig. 2).

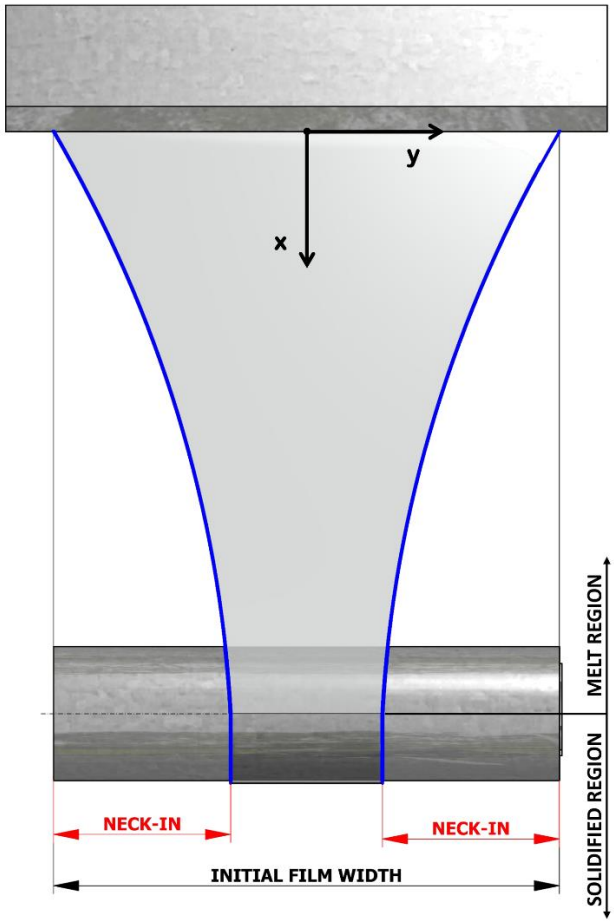

Fig. 2: Visualization of neck-in phenomenon during extrusion film casting.

To minimize the extent of neck-in phenomenon, a drawing length should be kept as short as possible (few centimeters in length) and wide flat die should be used. Neck-in magnitude is also severely impacted by viscoelastic properties of processed polymer melt. Theoretical predictions and numerical simulations

showed that the neck-in extent can be correlated with extensional viscosity hardening of the polymer melt [7–9].

1.2.2 Edge-beading

Beside the neck-in phenomenon, the interrelated defect termed as edge-beading or dog-bone defect is formed making the edge portions of the film substantially thicker than its central part (Fig. 3). The gauge of these elevated parts can be five times higher compared to the center and several centimeters wide. Predominant cause of edge-beads formation is edge-stress effect [10].

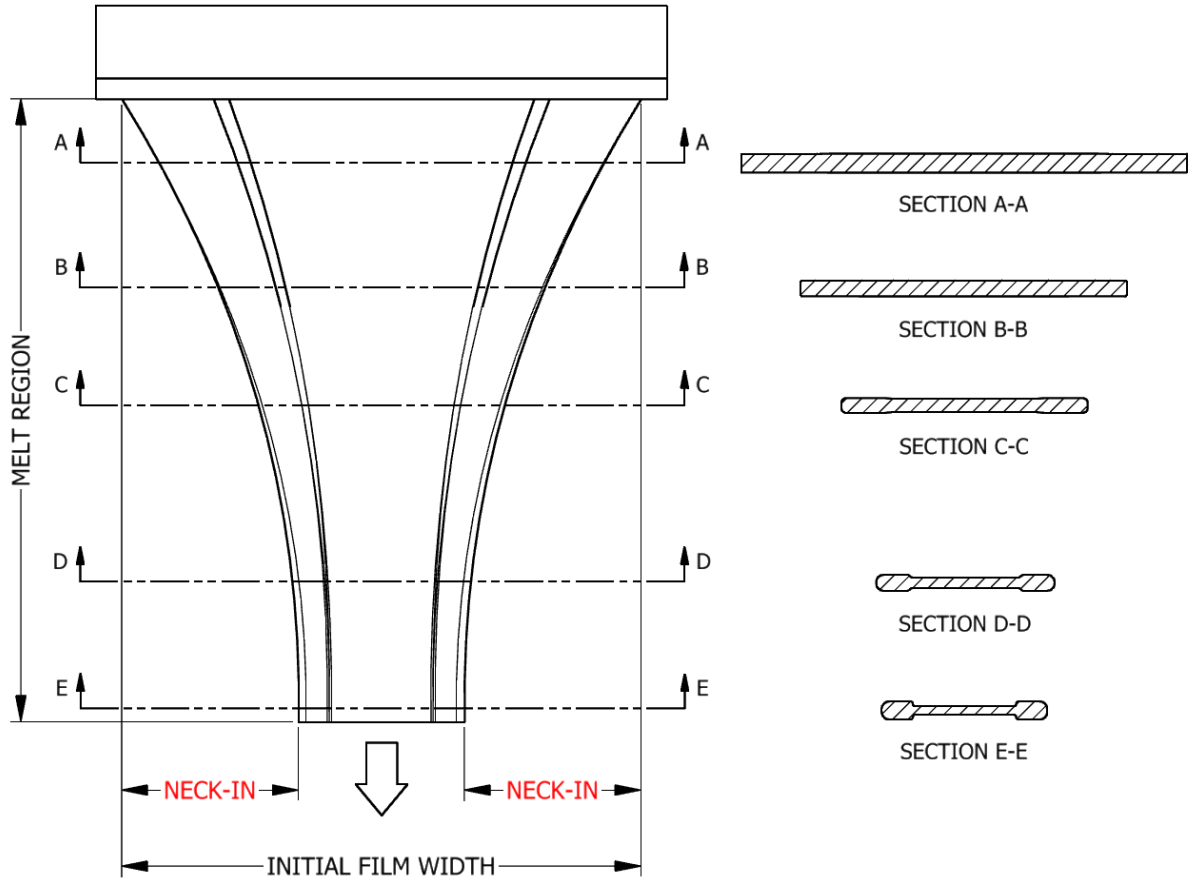

Fig. 3: Visualization of edge-beading phenomenon during extrusion film casting.

Consequently, those elevated edges are often trimmed by a slit razer, scrapped and potentially reprocessed in order to get even film surface. Disregard a large amount of waste material, there are another issue connected with edge-beads causing the air to be trapped between the film and chill roll resulting in turn to worse film quality. Even though formation of edge-beads represents a problem for reasons stated above and manufacturers make an effort to reduce them, their complete elimination might have a consequence in increased extent of neck-in phenomenon. Therefore, in the practice, the technological procedure can be found

when the formation of edge-beads is deliberately supported immediately after the polymer exits the die by the increased die lip opening at the ends of the slit die [4].

1.2.3 Draw Resonance

The stability of the process is considerable influenced by amount of stretching that is experienced by the film in the drawing zone. Thus, to evaluate the intensity of drawing in the take-up length, the draw ratio is introduced and since the take-up velocity is much greater than die exit velocity, its value is imposed higher than unity. The typical value of the draw ratio for the film casting operation is in range of 2 to 20 [4], albeit modern casting lines can operate in the much higher production rates. If the draw ratio achieves (for the given process conditions, die design and polymer used) some critical value, the transient hydrodynamic instability called draw resonance starts to occur, which may limit the processing window considerably.

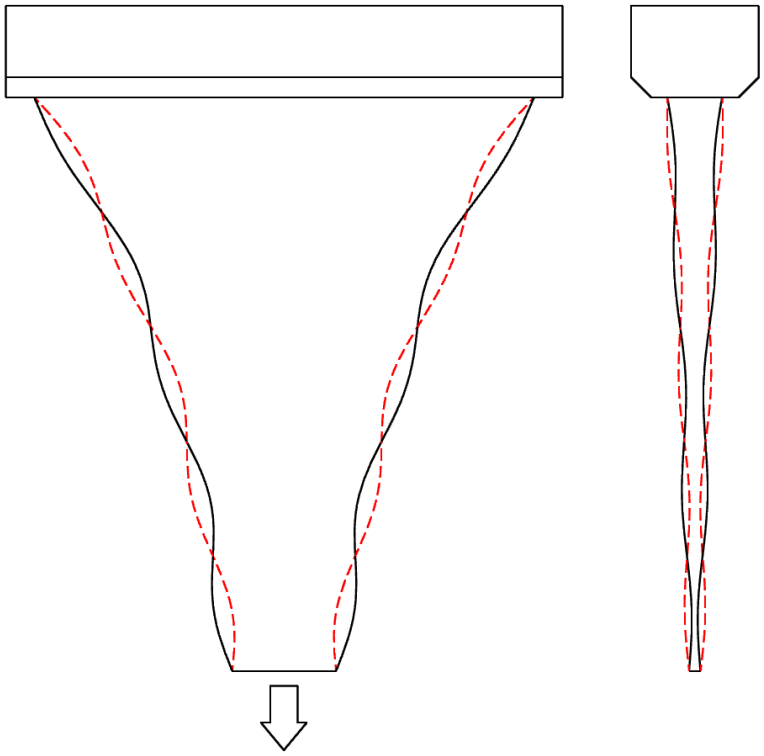

Fig. 4: Visualization of draw resonance experienced during extrusion film casting.

Among the signs of how this flow instability can be manifested belongs sustained oscillation in the film dimensions even though the volumetric flow supplied from the slit die and take-up speed is kept constant (Fig. 4). These sinusoidal oscillations of the same frequency in the film width and thickness (measured in the center of the film) are shifted to each other by the half-wave length (which is the maxima in width and corresponds to minima in thickness) and

vice versa [11]. However, it is worth to note that the results of numerical simulations suggests that the thickness disturbances in the central portion of the film are out-of-phase on par to those at edge part of the film and moreover, the oscillation amplitude is of higher value than that observed in thickness oscillation [12]. Lengthen drawing distance, increased cooling effects and utilization of polymers with strong extensional strain hardening behavior can stabilize process and shift the onset of draw resonance toward higher draw ratios.

Film breakage is another state that can be observed during the process of elevating draw ratio. In this case, the cohesive failure among the polymer chains causes the disintegration of the film if the critical in-film stress is exceeded due to the fact that chains cannot be longer reorganized in way to relieve local stresses in time frame imposed by the deformation. This can be seen in the polymers containing long chain branches or a high molecular weight portion that are processed in combination with high cooling rates in drawing zone, which results to good stability of the process but also in development of the high stretching stress [2].

2. Mathematical Modeling of the Extrusion Film Casting Process

2.1 Literature Review

Polymer sheet or filament drawing has received enormous amount of attention and been studied extensively over the past four decades both experimentally and theoretically (Tab. 1) due to its great importance in the polymer processing industry.

Table 1: Overview of steady-state analyses of film casting process (table adapted from [13–15] and updated for new studies).

Model Dimensionality	Viscous Fluids		Viscoelastic Fluids	
	Isothermal	Non-isothermal	Isothermal	Non-isothermal
1D	[16],[4],[17]	[6],[18],[19], [20],[21]	[22],[23], [24],[25], [26],[27]	[28],[29], [30],[31], [32], [33],[7],[8]
2D	[34]	[15],[35],[36]	[12],[37], [38],[39], [40],[30]	[41],[42],[43]
3D	[44]	[13]	[14]	

Initial efforts were made on a fiber spinning process for which the flow kinematics are similar from a mathematical point of view if considered as the one-dimensional flow case, for Newtonian and Maxwell fluids by Gelder [45] and Fisher [46, 47], respectively. Those studies were aimed on investigating the draw resonance phenomenon which was encountered for the first time by Christensen [48] and Miller [49], and who postulated that the nature of this phenomenon was not of viscoelastic nature because it could be observed in Newtonian fluids as well. Extending the process kinematics into two or three dimensions, the processes become different and one can observe phenomena in film casting that do not have a counterpart in fiber spinning, i.e. neck-in and edge-beading. The preliminary studies mentioned above provided the background for extended studies on EFC. Initial attempts to simulate EFC operations were dedicated to investigation of process stability and determination of draw resonance onset rather than to quantify the extent of neck-in phenomenon. The very first study on modeling of EFC process in this manner was carried out by Yeow [50] with utilization of numerical modeling. He used one-dimensional isothermal model for

Newtonian fluid (planar extensional free surface flow) for steady state solution and investigated the effect of introduced small two-dimensional perturbances on flow stability (namely transverse perturbations). The edge-effects, surface tension, aerodynamic drag and fluid inertia and gravity were neglected. A small curvature of the film together with uniform axial stress and axial velocity over film thickness were assumed. Due to the assumed kinematic in the free surface flow at the drawing section, the model could not capture an edge-bead defect and contraction in film width that was assumed to be infinitely wide. The Film thickness was allowed to vary in machine direction only.

Aird and Yeow [51] continued on this mathematical background for 1D model and extended analysis for power-law fluids. Consequently, Anturkar and Co [52] and Iyengar and Co [22, 53] utilized isothermal modified convected-Maxwell fluid and Giesekus constitutive equations for linear and non-linear analysis in simulations of viscoelastic fluids. First isothermal trials towards necking phenomena modeling were carried out by Sergent [54] and then by Cotto, Duffo and Barq [6, 18, 20] for non-isothermal conditions.

Another milestone work has been set by Dobroth and Erwin [10] who pointed out that the deformation flow in the drawing length comprises of two related regions and the extent of edge-beads and interrelated neck-in phenomenon is determined by the interplay between them through an edge stress effect. While the center of the film undergoes planar extensional deformation, the edge sections are subjected to uniaxial extensional one (see Fig. 5).

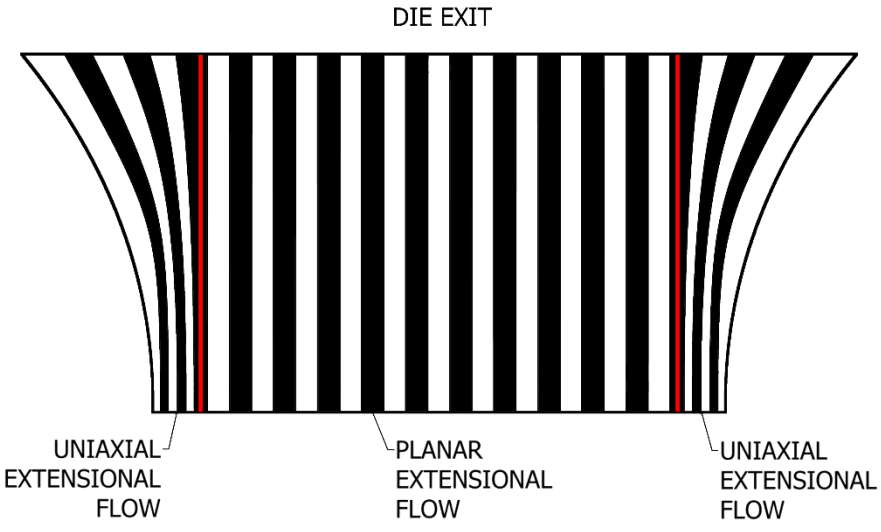

Fig. 5: Visualization of planar and uniaxial extensional flows during extrusion film casting.

In the case of fiber spinning, however, one can observe uniaxial extensional flow only. Some authors endeavored to relate and quantify the gauge of the

observed necking in terms of rheological parameters, such as shear, uniaxial and planar viscosity. Many authors reported that the strain hardening in uniaxial extensional viscosity may depress the extent of necking phenomena [37, 42, 55, 56]. This idea was continued by Ito [57], who related the neck-in extent to rheological parameters, such as the ratio of planar viscosities in axial and transverse directions, and derived an analytical equation for the edge line of a molten film of Newtonian and Maxwell fluid. Along the line of Dobroth and Erwin's article [10], who as the first recognized deformation type in the drawing area, Shiromoto [7, 8, 33], recently, presented the idea that the extent of the necking should not have been described by uniaxial extensional viscosity only in addition to take-up length but as the ratio of planar and uniaxial extensional viscosities reflecting the deformation type in the central and edge portion of the film in the drawing section. Aside from performing non-isothermal viscoelastic simulations, they also proposed a theoretical model based on force balance and deformation type of a film in order to predict necking behavior.

More recently, a 2D membrane model was presented by d'Halewyu [34] and Debbaut [37] for Newtonian and viscoelastic fluids, respectively. This frequently used model was capable of predicting the dog-bone defect, i.e. development of edge-beads, under the stationary conditions. Silagy et al. [58] proceeded forward and enriched the membrane model by a supplementary kinematic hypothesis that was originally brought by Narayanaswamy [59] in his paper on float glass stretching, and carried out an extended isothermal study on the influence of processing conditions on film geometry, and stability analysis of EFC for Newtonian and Maxwell fluid using the UCM constitutive equation. Because of the assumptions used in flow kinematics, this model was able to cover film width reduction and thus predict the neck-in phenomenon but was still not able to predict edge-beading. This limitation was removed in their succeeding work [12] where the 2D isothermal membrane model combined with PTT constitutive equation was developed and obtained steady and transient stability results compared with its 1D predecessor. In the following years, the 1D version of Sylagy's membrane model was used in many studies and considerable amount of work has been done on EFC under non-isothermal conditions including crystallization effects by Lamberti et al. [21, 60–62], Lamberti and Titomanlio [62–65], and Lamberti [66]. A three dimensional model for EFC simulation was further developed by Sakaki et al. [44]. The resolution of model equations required a utilization of finite element method. Problem was considered as an isothermal and steady state Newtonian flow. A process parameter space was chosen to reflect the industrial processing conditions. Model captured the development of both neck-in and edge beading and the effect of *DR*, *TUL* and die width were investigated. They found out that the gauge of neck-in and edge beading was affected by *DR* and *TUL* but not by the die width. The extent of neck-in increased with increasing *DR* and *TUL*. Lately, this approach was extended by Zheng et al. [13] for non-isothermal steady Newtonian fluid. Kometani et al. [9] conducted both an experimental and

theoretical investigation of effects of rheological properties on neck-in in film casting. For two tested materials PP and LDPE with no remarkable difference in the viscoelastic properties except the extensional ones (LDPE showed the remarkable increase in extensional viscosity at high strain rates), the neck-in extent for PP under the condition of higher draw ratio was increased over LDPE where neck-in was constant and independent of the draw ratio. Based on these experiments, the authors concluded that neck-in phenomenon in film casting depends on the extensional rheological properties. Furthermore, they utilized simulation based on three deferent rheological models (the Newtonian, Bird-Carreau and Giesekus model) with aim to evaluate its applicability to the film casting modeling. Results obtained from simulation based on Giesekus model were in quantitative agreement with experimental observation for both polymers, however, the other two utilized models did not provide a data good describing prediction due to their inaccurate expression in extensional viscosity.

The influence of macromolecular architecture on the extent of necking phenomenon has been investigated by Ito et al. [57, 67] (effects of draw ratio and take-up length on necking for LDPE, HDPE and mLLDPE) and Baird et al. [68, 69] (effects of long chain branching and molecular weight distribution on necking for LDPE, mLLDPE and Ziegler-Natta catalyzed LLDPE). Research on multi-layer film casting considering Giesekus fluid has been performed in studies of Pis-Lopez and Co for steady state [70] and stability analysis [71].

Recently, Pol et al. [23, 28] and Chikhalikar et al. [29] have published a series of articles in which they have performed experimental and theoretical investigations of the effects of long chain branching and molecular weight distribution on the necking phenomenon extent. For this purpose, they have utilized the 1D membrane model, originally proposed by Silagy [58], the multi-mode eXtended Pom-Pom constitutive equation and the multi-mode Rolie-Poly stretch constitutive equation, respectively, for the long chain branched (LDPE, PP) and the linear (HDPE, PP) polymers. Fixing the *DR* and *TUL*, they found that the extent of necking is lesser for HDPE with a broader molecular weight distribution than that for LLDPE with a narrower molecular weight distribution and further that long chain branched LDPE necks-in to lower extent than linear HDPE or LLDPE. In the succeeding study, Pol and Thete [30] switched from the one-dimensional model that was used in their predecessor works on this theme to the two-dimensional model which was originally proposed by Ito et al. [57] incorporating UCM constitutive equations. Additionally, they derived analytical solution for low and high Deborah numbers. They found that while the film width of modelled LLDPE continuously decreased with increased draw ratio, the film width for LDPE decreased with increased draw ratio in case of long take-up lengths and remained constant for shorter ones. That is, there is existence of a locus of points in the attainable region that divides *DR–De* plane into sections where the dependence of neck-in on draw ratio has opposite trends.

In their latest work [25], they addressed the effects of the individual viscoelastic relaxation modes of a polymer melt on its behavior in polymer melt extrusion film casting process using UCM and PTT constitutive equations and 1D isothermal membrane model. They found that experimental data for long-chain branched LDPE was described better by UCM model, whereas PTT model provided better simulation results for the linear LLDPE experimental data.

Even though, the real EFC manufacturing process involves complex kinematics and is considered as a 3D problem, whose numerical simulation can be very demanding, it has been proven by many authors that the EFC 1D membrane model (originally proposed by Silagy [58] and if used in combination with appropriate constitutive equations) is capable of providing results that are in good agreement with experiment data.

If viscoelastic constitutive equations are utilized, the additional boundary stress condition at the die exit must be specified. This boundary condition is given by both, flow in the die (upstream) and extensional flow in the drawing length (downstream). Thus, the accurate determination of this additional boundary stress value requires intensive numerical computation [72]. In the following paragraphs, a brief enumeration of approaches used in determination of these type of boundary conditions is provided.

Anturkar and Co [52] in their study, using modified convected Maxwell model, estimated axial component of stress tensor, τ_{xx}, as a mean stress value for fully-developed slit flow in a die of infinitely width. Silagy et al. [58] and [12] based on the works of Denn et al. [73] and Demay et al. [18, 74] assumed two different stress states at the end of the die. In the first case, an extra stress in machine direction, τ_{xx}, is equaled to zero and thus the extra stresses are entirely relaxed due to the die swell, or the second which assumed the mean value of extra stress after flow in an infinite die with a rectangular cross section while the transversal extra stress, τ_{yy}, is set to the value obtained from Newtonian solution. They found that initial stress conditions at the die have a little influence on the final film shape but the calculations were made only for low values of Deborah number. Iyengar and Co [22] have chosen different approach and instead of specifying axial stress component, they have set the ratio τ_{zz}/τ_{xx} at the value between two extreme cases for planar extensional flow and fully-developed slit flow in the die noting that the true stress ratio should have lied in their range. Iyengar [75] then reported that the both extreme cases with corresponding stress ratios provide very similar velocity and stress profiles. Debbaut at al. [37] in their viscoelastic study assumed initial stresses to be zero. Same as the approach in work of Smith [76].

For multilayer film casting analysis (based on the single-mode modified Giesekus model) Pis-Lopez and Co [70, 71] showed that if aspect ratio (defined

here as ratio of total film thickness at the die exit and drawing distance h_0/L) is less than 0.05, the velocity and stress profiles converge to the same values does not matter whether the initial stress condition is based on the assumption of fully-developed slit flow or fully-developed planar extensional flow. In another study, utilizing multi-mode model approach, Denn [77] left the longest relaxation mode unspecified at the die exit and rest of the modes was set up with respect to this mode. In contrary, Christodoulou et al. [72] drawn that the shortest mode should be left unspecified with the reasoning that the longest mode $\tau^{p}_{xx(N)}$ is mainly determined by the flow inside the die, whereas the shorter modes $\tau^{p}_{xx(j)}$ are determined by the external flow in the air gap.

Beris and Liu [78, 79], in their study on fiber spinning for single mode UCM viscoelastic liquid, specified a die exit stress state via stress ratio of the normal to the axial stress, τ_{yy}/τ_{xx}, and not each component separately. This value has been approximated as the value under homogeneous steady extensional flow at an effective extensional strain rate. For viscoelastic multimode model, Denn [77] specified also $\tau^{p}_{xx(j)}/\tau^{p}_{xx(N)}$ for j < N as extra condition to $\tau^{p}_{yy(j)}/\tau^{p}_{xx(j)}$ for all relaxation modes.

Devereux and Denn [80] suggested the same distribution among partial stresses as in the case of fully-developed capillary flow with neglected radial partial stresses. Remaining initial stresses were adjusted in order to meet the downstream boundary condition (see Eq. 2.1.1).

$$\frac{\tau^{p}_{xx(j)}}{\tau^{p}_{xx(N)}} = \frac{\lambda_j \mu_j}{\sum_{j=1}^{N} \lambda_j \mu_j} \tag{2.1.1}$$

Note that Gagon and Denn [81] simplified the aforementioned relation for wedge spectrum to form of

$$\frac{\tau^{p}_{xx(j)}}{\tau^{p}_{xx(N)}} = \frac{\lambda_j}{\lambda_N} \tag{2.1.2}$$

2.2 Mathematical models

Ideally, the proposed mathematical model should accommodate problem solution in three dimensions where all variables are dependent on all spatial coordinates and covers firstly, the development of the system over time, secondly, a non-isothermal conditions, thirdly, an influence of external forces (such as inertia and gravity) and finally, constitutive equations that can describe the

ultimate behavior of modelled polymer for given deformation and temperature history experienced by the polymer during the flow. The current problem is that consideration of all above mentioned factors in film casting modeling yields very complicated mathematical models, which cannot practically be solved by the existing mathematical tools. Therefore, different simplifying assumptions are applied to simplify the experimental reality leading to the film casting models that can be solved numerically in reasonable computational times. Those typical assumptions are provided bellow:

- Reduction in dimensionality: 1D, 1.5D and 2D;
- Isothermal conditions – constant temperature field
- Non-transient description
- Mechanically and thermally incompressible fluid
- Excluded effects of inertia
- Excluded effects of gravitational forces
- Constant boundary conditions
- Not realistic or simplified constitutive conditions
- Neglected aerodynamic drag
- Neglected surface tension
- Neglected die swell
- Neglected self-weight of the polymer
- Neglected edge-effects
- Excluded crystallization (temperature, flow-induced)
- Neglected the sag of film in non-vertical installations (film curvature)
- Effects from additional devices (air knife, vacuum box, electrostatic pinning)

2.2.1 One-dimensional Film Casting Model of Infinite Width

The first efforts to model extrusion film casting were dedicated to accommodate the basic behavior exhibited by a drawn polymer in the drawing zone [22, 50–52, 82]. This first approximation was based on an idea of the infinite film width. In this one-dimensional representation of flow kinematic, neck-in and edge-beading effects are not taken into account. Design of this model assumes that the velocity field can be described in the following way

$$\begin{aligned} v_x &= v_x(x,t) \\ v_y &= 0 \end{aligned} \qquad (2.2.1.3)$$

that is, the flow deformation in the drawing region is mainly planar.

Despite to this limitation, the one-dimensional model of infinite width can present a convenient framework for parametric studies with good approximation

of real cast lines where the die width is superior over the take-up length [10]. Responses of the system to the input changes, such as processing conditions or material parameters, might be more readily correlated to changes in the output, such as effects on film thickness or onset of draw resonance. Moreover, it can be stated in a close-form, especially for simple Newtonian fluids, thus its solution does not require employment of numerical tools.

2.2.2 One-dimensional Film Casting Model of Varying Width

To overcome limitation stemming from the assumptions taken for the infinite width model, one-dimensional film casting model with variable film width was proposed [12, 58]. This simplified model that retain the capability to cover film width reduction in drawing length at reduced dimensionality of resolved problem, is based on assumption that all velocity components are exclusive function of a position in a drawing length, *x*, at certain time, *t*, and vary linearly with respect to its corresponding direction.

Thus, velocity field is assumed in form of

$$\begin{aligned} v_x &= v_x(x,t) \\ v_y &= yf(x,t) \end{aligned} \qquad (2.2.2.4)$$

and continuity equation yields

$$v_z = -zg(x,t) \qquad (2.2.2.5)$$

However, based on the numerical simulations of Debbaut et al. [37] for viscoelastic fluids and experimental observations of Dobroth and Erwin [10], the flow in downstream is divided into regions where the central part of the film exhibits planar extensional flow whereas lateral part shows uniaxial extensional deformation flow that is not fully in compliance with taken assumption of linearly varied velocity component in thickness direction with thickness.

2.2.3 Two-dimensional Film Casting Model

The lower dimensional variants of film casting model can provide a reasonable estimate of draw resonance onset or neck-in phenomenon extent, if used with advanced constitutive equations, but cannot account for edge-bead formation. Therefore, the two-dimensional models having the ability to better describe a complex flow situation experienced by the polymer in drawing length were developed [34, 37]. Essential idea comes from the statement that the one dimension of the film is small in comparison to others [34], which is so-called the membrane hypothesis. Film thickness is much smaller than the film width and the take-up length, hence the velocity component in machine and transversal direction

can be assumed independent of thickness direction, that is, uniform across the thickness.

Then, the velocity field in the casted molten film can be written in form of

$$\begin{aligned} v_x &= v_x(x, y, t) \\ v_y &= v_y(x, y, t) \end{aligned} \tag{2.2.3.6}$$

and the continuity equation gives

$$v_z = -z\left(\frac{\partial v_x}{\partial x} + \frac{\partial v_y}{\partial y}\right) \tag{2.2.3.7}$$

THE AIMS OF THE DOCTORAL RESEARCH WORK

The major goal of the doctoral research work is to firstly, derive viscoelastic extrusion film casting model utilizing 1.5D membrane approximation, modified Leonov model as the constitutive equation and energy equation coupled with an advanced crystallization kinetic (considering thermally as well as stress induced crystallization) and secondly, to develop stable numerical scheme allowing to solve the proposed model in order to reveal the complicated relationship between polymer melt rheology, die design, process conditions and undesirable neck-in phenomenon. The key aims can be formulated as following:

- Validation of the proposed model predictions with literature experimental data for different polymer melts and processing conditions.

- Elucidate the role of planar to uniaxial extensional viscosity ratio, extensional strain hardening, Deborah number and die exit stress state (quantified via second to first normal stress difference ratio, $-N_2/N_1$) on the neck-in phenomenon.

- Quantification of the neck-in phenomenon via a simple dimensionless analytical equation.

- Investigation the role of heat transfer coefficient, draw ratio, die exit temperature and flow induced crystallization on the production of flat polymeric membranes with specific attention to neck-in phenomenon.

3. Viscoelastic Modeling of Non-isothermal Extrusion Film Casting Process Considering Temperature and Stress Induced Crystallization

3.1 Modified Leonov Model

The utilized constitutive equation is based on heuristic thermodynamic arguments resulting from the theory of rubber elasticity [83–88]. In this approach, a fading memory of the melt is determined through an irreversible dissipation process driven by the dissipation term, *b*. From mathematical viewpoint, it is relating the stress and elastic strain stored in the material as:

$$\underline{\underline{\tau}} = 2\left(\underline{\underline{c}} \cdot \frac{\partial W}{\partial I_{1,c}} - \underline{\underline{c}}^{-1} \cdot \frac{\partial W}{\partial I_{2,c}} \right) \tag{3.1.8}$$

where $\underline{\underline{\tau}}$ is the stress, and *W*, the elastic potential, which depends on the invariants $I_{1,c}$ and $I_{2,c}$ of the recoverable Finger tensor, $\underline{\underline{c}}$,

$$W = \frac{3G}{2(n+1)} \left\{ [1-\beta] \cdot \left[\left(\frac{I_{1,c}}{3} \right)^{n+1} - 1 \right] + \beta \left[\left(\frac{I_{2,c}}{3} \right)^{n+1} - 1 \right] \right\} \tag{3.1.9}$$

where *G* denotes linear Hookean elastic modulus, β and *n* are numerical parameters. Leonov assumed that the dissipative process acts to produce an irreversible rate of strain, $\underline{\underline{e}}_p$

$$\underline{\underline{e}}_p = b\left[\underline{\underline{c}} - \frac{I_{1,c}}{3} \underline{\underline{\delta}} \right] - b\left[\underline{\underline{c}}^{-1} - \frac{I_{2,c}}{3} \underline{\underline{\delta}} \right] \tag{3.1.10}$$

which spontaneously reduces the rate of elastic strain accumulation. Here, $\underline{\underline{\delta}}$ is the unit tensor and *b* stands for dissipation function defined by Eq. 3.1.12. This elastic strain, $\underline{\underline{c}}$, is related to the deformation rate tensor, $\underline{\underline{D}}$, as follows

$$\overset{\circ}{\underline{\underline{c}}} - \underline{\underline{c}} \cdot \underline{\underline{D}} - \underline{\underline{D}} \cdot \underline{\underline{c}} + 2\underline{\underline{c}} \cdot \underline{\underline{e}}_p = 0 \tag{3.1.11}$$

where $\overset{\circ}{\underline{\underline{c}}}$ is the Jaumann (corotational) time derivative of the recoverable Finger strain tensor. In this work, the Mooney potential (i.e. n=0 in Eq. 3.1.9), and the dissipation function, *b*, proposed in [89] (see Eq. 3.1.12) have been employed.

$$b\left(I_{1,c}\right)=\frac{1}{4\lambda}\left\{\exp\left[-\xi\sqrt{I_{1,c}-3}\right]+\frac{\sinh\left[\nu\left(I_{1,c}-3\right)\right]}{\nu\left(I_{1,c}-3\right)+1}\right\} \tag{3.1.12}$$

Here, ξ and ν are adjustable model parameters.

$$I_{1,c}=\mathrm{tr}\left(\underline{\underline{c}}\right) \tag{3.1.13}$$

$$\mathrm{tr}\left(\underline{\underline{c}}\right)=c_{xx}+c_{yy}+c_{zz} \tag{3.1.14}$$

$$I_{2,c}=\frac{1}{2}\left\{\left[\mathrm{tr}\left(\underline{\underline{c}}\right)\right]^2-\mathrm{tr}\left(\underline{\underline{c}}^2\right)\right\} \tag{3.1.15}$$

$$I_{2,c}=c_{xx}^{-1}+c_{yy}^{-1}+c_{zz}^{-1} \tag{3.1.16}$$

Differentiating Eq. 3.1.9 with respect to the first and second invariant of the recoverable Finger tensor yields

$$\frac{\partial W}{\partial I_{1,c}}=\frac{1}{2}G\left(\frac{I_{1,c}}{3}\right)^n\left(1-\beta\right) \tag{3.1.17}$$

$$\frac{\partial W}{\partial I_{2,c}}=\frac{1}{2}G\beta\left(\frac{I_{2,c}}{3}\right)^n \tag{3.1.18}$$

Combination of Eq. 3.1.8 with Eqs. 3.1.17–3.1.18 leads to the following expression for the extra stress tensor.

$$\underline{\underline{\tau}}=G\left\{\underline{\underline{c}}\left[\left(\frac{I_{1,c}}{3}\right)^n\left(1-\beta\right)\right]-\underline{\underline{c}}^{-1}\left[\beta\left(\frac{I_{2,c}}{3}\right)^n\right]\right\} \tag{3.1.19}$$

3.2 Membrane Model of Film Casting

In this Ph.D. thesis, the 1.5D membrane model developed by Silagy et al. [58] was used as the basic to model the extrusion film casting process. The model essentially features two hypotheses to facilitate the description of the stress and velocity field development in the film drawing. Firstly, the total stress in the film thickness direction is assumed to be equal to zero because this dimension is small compared to other dimensions and secondly, velocities in the width and thickness direction are allowed to vary linearly with *y* and *z* position, respectively, for the given *x* location, which represents a supplementary kinematic hypothesis

(formerly adopted in the work of Narayanaswamy [59] for the modeling of glass manufacturing by the float process) in order to reduce the dimensionality of the task. Even though, the dimensionality of the model can be considered as a unity (all model variables are x-direction dependent only), it possess the capability to predict both, the reduction in film thickness as well as film width shrinkage. From this point of view, the model might be considered as a pseudo 2D or 1.5D.

Furthermore, the inertia, gravity, surface tension and aerodynamic drag are neglected in this model because they are usually much smaller in comparison with the stresses generated in the viscoelastic polymer melt. Finally, the original membrane model for EFC is based on the assumption of process isothermality, which can be justifiable for small enough drawing lengths and/or very high draw-down speeds [19]. However, this assumption seems to be false under processing conditions, where the melt has enough time to cool down, i.e. fabrication of porous membranes [90–94]. Therefore, in this work, the process is treated as a non-isothermal considering a thermally induced crystallization as well as flow induced crystallization. The detailed description of the utilized model is provided below.

3.2.1 Velocity Field

The Cartesian system axes are directed as follows (Fig. 1): in-film-plane axes *x* and *y*, where *x* points in the streamwise direction and *y* is perpendicular onto it, and *z* axis is normal to the film *xy* plane with origin deployment in the cross-sectional center of gravity at the die exit. The dimensions of the film are denoted as follows: take up length is X, initial film half-width is L_0, and initial half-thickness is e_0. The intensity of film drawing is expressed in terms of draw ratio (DR) that relates the final tangential velocity of the film at the chill roll, $u(X)$, to the film velocity at the die exit, u_0. The quantities without a zero subscript denotes non-initial corresponding dimensions at any given x position. The influence of extrudate swelling on the casting process is assumed to be negligible here. Using the symmetry of the problem and the kinematic hypothesis, the complexity of the velocity field involved in the film drawing is reduced, where each of the components is the function of all spatial and time variables. In the resulting form, the velocity field for steady solution is approximated as follows:

$$\begin{aligned} u &= u(x) \\ v &= v(x, y) = yf(x) \\ w &= w(x, z) = zg(x) \end{aligned} \qquad (3.2.1.20)$$

where u, v and w are the velocity components in the machine, transverse, and thickness direction, respectively. The deformation rate tensor, which is based on Eq. 3.2.1.20, takes the following form:

$$\underline{\underline{D}} = \begin{bmatrix} \frac{du}{dx} & \frac{1}{2}y\frac{df}{dx} & \frac{1}{2}z\frac{dg}{dx} \\ \frac{1}{2}y\frac{df}{dx} & f(x) & 0 \\ \frac{1}{2}z\frac{dg}{dx} & 0 & g(x) \end{bmatrix} \tag{3.2.1.21}$$

Since the polymer flow in EFC is mainly extensional and in an effort to increase simplicity, the shear rate components can be neglected in favor of extensional ones in Eq. 3.2.1.21, which leads to the following final expression for the deformation rate tensor:

$$\underline{\underline{D}} = \begin{bmatrix} \frac{du}{dx} & 0 & 0 \\ 0 & f(x) & 0 \\ 0 & 0 & g(x) \end{bmatrix} \tag{3.2.1.22}$$

The film thickness is constant throughout the film width due to the assumed velocity field, where the *v* and *w* velocity components are dependent on *x* variable only and are allowed to vary linearly over the film width and thickness, respectively, due to the applied Narayanaswamy's supplementary kinematic hypothesis as mentioned above.

3.2.2 Continuity Equation

The continuity equation requires the conservation of mass at any given streamwise position and with the incompressibility hypothesis takes the following form.

$$\frac{d}{dt}(eL) + \frac{d}{dx}(eLu) = 0 \tag{3.2.2.23}$$

Since the transient solution of the equation is not an objective of this study, the derivative with respect to time can be neglected. For steady state solution, the derivative with respect to time is

$$\frac{d}{dt}(eL) = 0 \tag{3.2.2.24}$$

and thus, the volumetric flow rate at the die exit position and at any given streamwise position is given by Eq. 3.2.2.25 and Eq. 3.2.2.26, respectively.

$$e_0 L_0 u_0 = Q \tag{3.2.2.25}$$

$$e(x)L(x)u(x) = Q \tag{3.2.2.26}$$

It is important to mention that the volumetric flow rate *Q* here corresponds to 1/4th of the cross-section only due to the process symmetry as show in [32].

3.2.3 Momentum Conservation Equation

Considering the membrane approximation for the thin film in the presence of a constant drawing force, the stresses are constant over the cross section of the film, which leads to the force balance having the following form

$$\frac{d}{x}\left(\sigma_{xx} L e\right) = \frac{dF}{dx} = 0 \tag{3.2.3.27}$$

Neglecting gravity, inertia, aerodynamic friction and surface tension forces, the drawing force becomes x-direction independent, which is fully balanced by the stresses generated in the film.

$$F = const = \sigma_{xx} L e \tag{3.2.3.28}$$

In this equation, σ_{xx} stands for the first diagonal component of the total stress tensor, $\underline{\underline{\sigma}}$, which is defined via the extra stress tensor, $\underline{\underline{\tau}}$, as follows

$$\underline{\underline{\sigma}} = -p\underline{\underline{\delta}} + \underline{\underline{\tau}} = \begin{bmatrix} -p + \tau_{xx} & 0 & 0 \\ 0 & -p + \tau_{yy} & 0 \\ 0 & 0 & -p + \tau_{zz} \end{bmatrix} \tag{3.2.3.29}$$

where *p* stands for the isotropic pressure, $\underline{\underline{\delta}}$ is the unity tensor. As it can be seen from Eq. 3.2.3.29, the diagonal components of the total stress tensor are defined as

$$\begin{aligned} \sigma_{xx} &= -p + \tau_{xx} \\ \sigma_{yy} &= -p + \tau_{yy} \\ \sigma_{zz} &= -p + \tau_{zz} \end{aligned} \tag{3.2.3.30}$$

The membrane approximation requires zero value of the thickness-wise component of total stress tensor, $\sigma_{zz} = 0$, which leads to

$$0 = -p + \tau_{zz} \tag{3.2.3.31}$$

i.e.

$$\tau_{zz} = p \tag{3.2.3.32}$$

Substituting Eq. 3.2.3.32 back into expression for stress components Eq. 3.2.3.30, the hydrostatic pressure term is eliminated, which leads to the following final expression for the diagonal components of the total stress tensor

$$\begin{aligned} \sigma_{xx} &= \tau_{xx} - \tau_{zz} \\ \sigma_{yy} &= \tau_{yy} - \tau_{zz} \\ \sigma_{zz} &= 0 \end{aligned} \tag{3.2.3.33}$$

After substitution of σ_{xx}, which is given by Eq. 3.2.3.33, into Eq. 3.2.3.28, the final form of the force balance equation is obtained

$$\left(\tau_{xx} - \tau_{zz}\right) Le = F \tag{3.2.3.34}$$

3.2.4 The Stress-free Surface Boundary Condition

Assuming the surface tension and air drag are negligible, the net force per unit surface at the film free surface is equal to zero:

$$\underline{\underline{\sigma}} \cdot \underline{n} = 0 \tag{3.2.4.35}$$

where the $\underline{n}$ is the unit vector normal to the free film surface. This yields the following expression relating the stress state of the film with the film half-width at given x position:

$$\left(\frac{dL}{dx}\right)^2 = \frac{\sigma_{yy}}{\sigma_{xx}} \tag{3.2.4.36}$$

3.2.5 The Kinematic Free-surface Boundary Condition

The fluid is enclosed in the boundaries of the free surface, which can be expressed as

$$\underline{u} \cdot \underline{n} = 0 \tag{3.2.5.37}$$

where $\underline{u}$ is the tangential velocity at the film-air interface. Combination of Eq. 3.2.5.37 with the equation of continuity leads to

$$u(x)\frac{dL}{dx} - f(x)L = 0 \tag{3.2.5.38}$$

$$u(x)\frac{de}{dx} - g(x)e = 0 \tag{3.2.5.39}$$

where $f(x)$ and $g(x)$ are components of the deformation rate tensor (see Eq. 3.2.1.22) in the width and thickness direction, respectively, which can simply be expressed as

$$f(x) = \frac{u(x)}{L}\frac{dL}{dx} \tag{3.2.5.40}$$

$$g(x) = \frac{u(x)}{e}\frac{de}{dx} \tag{3.2.5.41}$$

3.2.6 Dimensionless Transformation

For the sake of simplicity and scaling purposes, the dimensionless transformation has been introduced into the previously derived equations (having similar form as in [58]). Corresponding dimensionless quantities are denoted here with the overline symbol. Dimensionless transformation for the extra stress tensor and total stress tensor is defined here as

$$\overline{\tau}_{ii} = \frac{\tau_{ii} e_0 L_0}{F} \tag{3.2.6.42}$$

$$\overline{\sigma}_{ii} = \frac{\sigma_{ii} e_0 L_0}{F} \tag{3.2.6.43}$$

whereas the dimensionless spatial dimensions and streamwise velocity component are

$$\overline{x} = \frac{x}{X} \tag{3.2.6.44}$$

$$\overline{e} = \frac{e}{e_0} \tag{3.2.6.45}$$

$$\overline{L} = \frac{L}{L_0} \tag{3.2.6.46}$$

$$\bar{u} = \frac{u}{u_0} \tag{3.2.6.47}$$

Dimensionless numbers, such as draw ratio, *DR*, Deborah number, *De*, aspect ratio, *A*, and dimensionless force, *E*, are defined as follows

$$DR = \frac{u(X)}{u_0} \tag{3.2.6.48}$$

$$De = \frac{\lambda u_0}{X} \tag{3.2.6.49}$$

$$A = \frac{X}{L_0} \tag{3.2.6.50}$$

$$\frac{1}{E} = \frac{FX}{G\lambda e_0 L_0 u_0} \tag{3.2.6.51}$$

Introducing the dimensionless transformation into the continuity equation (Eq. 3.2.2.26) and momentum conservation equation (Eq. 3.2.3.34) leads to the following dimensionless implicit forms

$$\bar{e}\bar{L}\bar{u} = 1 \tag{3.2.6.52}$$

$$\left(\bar{\tau}_{xx} - \bar{\tau}_{zz}\right)\bar{L}\bar{e} = 1 \tag{3.2.6.53}$$

Substitution of Eq. 3.2.6.52 into Eq. 3.2.6.53 gives

$$\left(\bar{\tau}_{xx} - \bar{\tau}_{zz}\right) - \bar{u} = 0 \tag{3.2.6.54}$$

and differentiating Eq. 3.2.6.52 and Eq. 3.2.6.54 with respect to *x* variable, one can obtain

$$\frac{1}{\bar{e}}\frac{d\bar{e}}{d\bar{x}} + \frac{1}{\bar{L}}\frac{d\bar{L}}{d\bar{x}} + \frac{1}{\bar{u}}\frac{d\bar{u}}{d\bar{x}} = 0 \tag{3.2.6.55}$$

$$\frac{d\bar{\tau}_{xx}}{d\bar{x}} - \frac{d\bar{\tau}_{zz}}{d\bar{x}} - \frac{d\bar{u}}{d\bar{x}} = 0 \tag{3.2.6.56}$$

After rearrangement, the derivative of the dimensionless film half-thickness and axial velocity with respect to *x* are finally defined as

$$\frac{d\bar{e}}{d\bar{x}} = -\left(\frac{1}{\bar{L}} \frac{d\bar{L}}{d\bar{x}} + \frac{1}{\bar{u}} \frac{d\bar{u}}{d\bar{x}} \right) \bar{e} \tag{3.2.6.57}$$

$$\frac{d\bar{u}}{d\bar{x}} = \frac{d\bar{\tau}_{xx}}{d\bar{x}} - \frac{d\bar{\tau}_{zz}}{d\bar{x}} \tag{3.2.6.58}$$

The dimensionless forms for $f(x)$ and $g(x)$ functions, which were derived from the kinematic free-surface boundary condition and appear in the deformation rate tensor, are the following

$$\bar{f} = \frac{L_0}{u_0} f(x) \tag{3.2.6.59}$$

$$\bar{g} = \frac{e_0}{u_0} g(x) \tag{3.2.6.60}$$

Finally, the dimensionless transformation for the x-direction derivative of the film half-width (arising from Eq. 3.2.3.33 and Eq. 3.2.4.36) yields

$$\frac{d\bar{L}}{d\bar{x}} = -A \sqrt{\frac{\bar{\tau}_{yy} - \bar{\tau}_{zz}}{\bar{\tau}_{xx} - \bar{\tau}_{zz}}} \tag{3.2.6.61}$$

3.2.7 Extrusion Film Casting Model for the Modified Leonov Model

To combine the modified Leonov constitutive equation and the extrusion film casting model equations, it is necessary to derive the equation for particular stress development along the x axis. The relationship between the dimensionless stress and the recoverable strain, imposed from the modified Leonov model (Eqs. 3.1.8 and 3.1.19), can be described by the following formula (for the case of the Mooney potential, i.e. when n=0 and $\beta \neq 0$):

$$\bar{\tau}_{ii} = \frac{E}{De} c_{ii} - \frac{E}{De} c_{ii} \cdot \beta - \frac{E}{De} c_{ii}^{-1} \cdot \beta \tag{3.2.7.62}$$

Differentiating this equation with respect to *x* leads to

$$\frac{d\bar{\tau}_{ii}}{d\bar{x}} = \frac{E}{De} \frac{dc_{ii}}{d\bar{x}} - \frac{E}{De} \beta \frac{dc_{ii}}{d\bar{x}} - \frac{E}{De} \beta \left(-\frac{1}{c_{ii}^2} \frac{dc_{ii}}{d\bar{x}} \right) \tag{3.2.7.63}$$

where $dc_{ii}/d\bar{x}$ stands for the x-direction derivative of the recoverable strain tensor. This term is defined by Eq. 3.1.11 and for each component of the recoverable strain tensor it takes the following form:

$$\frac{dc_{xx}}{d\bar{x}} = 2c_{xx}\frac{1}{\bar{u}}\frac{d\bar{u}}{d\bar{x}} - \frac{2\bar{b}}{\bar{u}}Z_x \tag{3.2.7.64}$$

$$\frac{dc_{yy}}{d\bar{x}} = 2c_{yy}\frac{1}{\bar{L}}\frac{d\bar{L}}{d\bar{x}} - \frac{2\bar{b}}{\bar{u}}Z_y \tag{3.2.7.65}$$

$$\frac{dc_{zz}}{d\bar{x}} = 2c_{zz}\frac{1}{\bar{e}}\frac{d\bar{e}}{d\bar{x}} - \frac{2\bar{b}}{\bar{u}}Z_z \tag{3.2.7.66}$$

where $\bar{b}$, Z_i and X_p are defined as

$$\bar{b}\left(I_{1,c}\right) = \frac{1}{4De}\left\{\exp\left[-\xi\sqrt{I_{1,c}-3}\right] + \frac{\sinh\left[\nu\left(I_{1,c}-3\right)\right]}{\nu\left(I_{1,c}-3\right)+1}\right\} \tag{3.2.7.67}$$

$$Z_i = c_{ii}\left(c_{ii} - c_{ii}^{-1} + X_p\right) \tag{3.2.7.68}$$

$$X_p = \frac{1}{3}\left(c_{xx}^{-1} + c_{yy}^{-1} + c_{zz}^{-1} - c_{xx} - c_{yy} - c_{zz}\right) \tag{3.2.7.69}$$

Combination of Eq. 3.2.6.58 and Eq. 3.2.7.63 leads to the dimensionless streamwise deformation rate, which takes the following form

$$\frac{d\bar{u}}{d\bar{x}} = \frac{\begin{array}{l}\bar{b}\left[\beta\left(Z_x - Z_z\right) - Z_x + Z_z\right] + \\ +\bar{b}\beta\left(\frac{1}{c_{zz}^2}Z_z - \frac{1}{c_{xx}^2}Z_x\right) + \frac{\bar{u}}{\bar{L}}\frac{d\bar{L}}{d\bar{x}}\left(c_{zz}\left(1-\beta\right) + \frac{\beta}{c_{zz}}\right)\end{array}}{\beta\left(c_{xx}+c_{zz}\right) - c_{xx} - c_{zz} - \frac{\beta}{c_{xx}}\left(\frac{c_{zz}+c_{xx}}{c_{zz}}\right) + \frac{De\bar{u}}{2E}} \tag{3.2.7.70}$$

Listed equations in sections 3.2.1–3.2.7 represent the basic isothermal viscoelastic 1.5D membrane model based on constitutive equation of the Leonov model. In order to enhance model into a non-isothermal variant with capability to predict crystallization, the energy equation with an appropriate crystallization kinetics has to be incorporated as described in the following paragraph.

3.2.8 Energy Equation

The energy balance equation [21] takes the following form and accounts for the temperature change, crystallinity and flow dependency of melt viscosity.

$$\frac{dT}{dx} = \frac{2HTC\left(T_a - T\right)L}{C_p \dot{m}} + \frac{\Delta H}{C_p}\frac{dX_c}{dx} \tag{3.2.8.71}$$

where, the *L(x)* is film half-width, *HTC* is heat transfer coefficient, C_p is specific heat capacity, $\dot{m}$ is mass flow rate in quarter-cross-section, ΔH is latent heat of crystallization, *T(x)* and T_a is melt and ambient air temperature, respectively, and finally $X_c(x)$ stands for content of crystallinity in the polymer volume. Heat transfer coefficient was chosen to be a constant in this model as a simplification representing a total heat exchange with the surrounding environment. The temperature dependence of melt relaxation time, λ, is described by Arrhenius form with a constant activation energy E_a as follows

$$\lambda = \alpha_T \lambda_0 \tag{3.2.8.72}$$

$$\alpha_T = \exp\left[\frac{E_a}{R}\left(\frac{1}{T} - \frac{1}{T_r}\right)\right] \tag{3.2.8.73}$$

where λ_0 denotes melt relaxation time at the die exit, *R* is universal gas constant and T_r is reference melt temperature.

Crystallization kinetics

The crystallization kinetics model adopted in this doctoral thesis was originally drawn by Ziabicki [95, 96] and later modified by Lamberti [97]. The quiescent conditions are defined as

$$T_m = T_{mq}^0 \tag{3.2.8.74}$$

On condition that, the flow induced crystallization is not included, the polymer melting temperature and flow induced equilibrium melting temperature are equal.

The volume fraction of crystallized phase, χ_c, and function *P(t)* expressing the non-linear description of crystallinity evolution, derived according time as

$$\chi_c(t) = \frac{X_c(t)}{X_{eq}} = 1 - \exp\left\{-\left[P(t)\right]^{n_c}\right\} \tag{3.2.8.75}$$

where *K(t)* is crystallization kinetics constant representing crystallization rate, X_{eq} is the equilibrium volume content of crystallinity (maximum in a crystal phase

that melt can possess) and constant n_c stands for a type of nucleation and crystal evolution. After differentiation with respect to time, the time-evolution formula is

$$\frac{dX_c(t)}{dt} = -X_{eq}\exp\left\{-\left[P(t)\right]^{n_c}\right\}\left\{-n\left[P(t)\right]^{n_c-1}\right\}\frac{dP(t)}{dt} \qquad (3.2.8.76)$$

In the simplified form, the model kinetics proposed by Ziabicki [95, 96] and adopted in this work is as follows

$$K(t) = \frac{d}{dt}P(t) \qquad (3.2.8.77)$$

$$K = K_{th}\left(1+\dot{T}Z\right)^{1/n_c} \qquad (3.2.8.78)$$

Here, K_{th} term is responsible for the low cooling rate crystallization, κ_1, κ_2 and E_c are material parameters determined from isothermal test, R is gas constant and T_{mq}^{0} denotes equilibrium crystallization temperature. B_{ath} and A_{ath} are material parameters included into the model by Lamberti considering the cooling history and promoting the model to be capable to describe a crystallinity evolution at high cooling rates.

$$K_{th} = \kappa_1\frac{T(T_m-T)}{(T_m)^2}\exp\left[-\frac{E_c}{RT}\right]\exp\left[-\kappa_2\frac{(T_m)^2}{T(T_m-T)}\right] \qquad (3.2.8.79)$$

Effect of cooling rate on crystallization kinetics constant is covered by non-isothermal function, Z, taking form of

$$Z = -B_{ath}\left|\dot{T}\right|^{A_{ath}}\frac{(T_m)^5}{T(T_m-T)^5}\exp\left[\frac{E_c}{RT}\right] \qquad (3.2.8.80)$$

where, cooling rate is marked as $\dot{T}$, the derivative of the film temperature with respect to time, t. The formula for the transition from time to spatial coordinates is following

$$\dot{T} = \frac{dT}{dt} = u\frac{dT}{dx} \qquad (3.2.8.81)$$

After its application on Eq. 3.2.8.76 with dimensionless transformation introduced in section 3.2.6 and rearrangement, the final form of equation for the crystallinity evolution in dimensionless spatial coordinates demands

$$\frac{dX_c(\bar{x})}{d\bar{x}} = X_{eq}\exp\left\{-\left[P(\bar{x})\right]^{n_c}\right\}n_c\left[P(\bar{x})\right]^{n_c-1}\frac{dP(\bar{x})}{d\bar{x}}\frac{X}{\bar{u}u_0} \qquad (3.2.8.82)$$

and semi-dimensionless form of energy equation, Eq. 3.2.8.71, is then given as

$$\frac{dT}{d\bar{x}} = \frac{2HTC\left(T_a - T\right)\bar{L}X}{C_p\dot{m}} + \frac{\Delta H}{C_p}\frac{dX_c}{d\bar{x}} \tag{3.2.8.83}$$

Effect of crystallinity on viscosity

Beside the effect of temperature on the melt relaxation time, the effect of crystallinity on viscosity is included into the model through the function μ_{Xc} that acts directly on the initial elastic modulus G_0; this approach was presented by Titomanlio in [98].

$$G = \mu_{X_c}\left(X_c\right)G_0 \tag{3.2.8.84}$$

This S-shaped function remains unity as the amount of crystallinity in volume is low and at the certain point starts to deviate and sharply raise simulating the phase transition from melt to the solid state:

$$\mu_{X_c}\left(X_c\right) = 1 + f\exp\left(-\frac{h}{X_c^m}\right) \tag{3.2.8.85}$$

It is worth to note that Eq. 3.2.6.54 is no more globally satisfied as in the original model proposal [58] where modulus G was taken as a constant and from now on must be treated as follows

$$\int_0^{\bar{\tau}_{xx}(X)} d\bar{\tau}_{xx} - \int_0^{\bar{\tau}_{zz}(X)} d\bar{\tau}_{zz} - \int_0^{\bar{u}(X)} d\bar{u} = 0 \tag{3.2.8.86}$$

Flow-induced crystallization

Effect of flow on crystallization is described via molecular strain that increases both growth and nucleation rates. In the used formulation [99], melting temperature is continuously modified according to the current molecular strain as follows

$$T_m(S_F) - T_{mq}^0 = \frac{1}{2}\left[\tanh\left(\frac{S_F - A_1}{A_2}\right) + 1\right]\left(A_3S_F + A_4\right) \tag{3.2.8.87}$$

where T_{mq}^0 and $T_m(S_F)$ is equilibrium and quiescent melting temperature, and $A_{1\text{-}4}$ are experimentally determined parameters, S_F is stretch function expressed here in the following form

$$S_F = I_{1,c} - 3 \tag{3.2.8.88}$$

In the proposed formula, the molecular stretch is measured over the first invariant of recoverable Finger tensor $I_{1,c}$.

3.2.9 Boundary Conditions

The complex and essential explicit model equations constituted in the previous section, namely Eqs. 3.2.6.57, 3.2.6.61, 3.2.7.70, 3.2.7.64, 3.2.7.65, 3.2.7.66 has to be solved with the appropriate set of the boundary conditions. Detailed description of the utilized boundary conditions is provided below.

Upstream boundary conditions:

Taking advantage of the dimensionless transformation, the initial half-width, half-thickness, and streamwise velocity are equal to one.

$$\bar{u}(0)=1 \tag{3.2.9.89}$$

$$\bar{e}(0)=1 \tag{3.2.9.90}$$

$$\bar{L}(0)=1 \tag{3.2.9.91}$$

Due to the employment of the energy equation together with crystallization kinetics equation, two additional conditions for initial melt temperature and crystallinity content (assumed to be a zero) are invoked.

$$T(0)=T_{DIE} \tag{3.2.9.92}$$

$$X_c(0)=0 \tag{3.2.9.93}$$

Since a viscoelastic constitutive equation is involved in this study, it is necessary to define initial boundary conditions for all three diagonal components of the extra stress tensor $\bar{\tau}_{xx}(0)$, $\bar{\tau}_{yy}(0)$ and $\bar{\tau}_{zz}(0)$ by using Eq. 3.2.7.62. To do that, diagonal components of the recoverable strain tensor at the die exit must be determined as the first by solving the following set of equations

$$\frac{E}{De}\left[\left(c_{xx}-c_{zz}\right)(1-\beta)+\beta\left(c_{zz}^{-1}-c_{xx}^{-1}\right)\right]-1=0 \tag{3.2.8.94}$$

$$c_{xx}c_{yy}c_{zz}=1 \tag{3.2.8.95}$$

$$-\frac{N_2}{N_1}=-\frac{E\left[c_{zz}-c_{yy}+\beta\left(c_{yy}+c_{yy}^{-1}-c_{zz}-c_{zz}^{-1}\right)\right]}{De\bar{u}} \tag{3.2.8.96}$$

Eq. 3.2.8.94 arises from the momentum conservation equation 3.2.3.34 by combination of Eqs. 3.2.6.54, 3.2.7.62 and 3.2.9.89 whereas Eq. 3.2.8.95 represents the incompressibility condition for the given flow situation. Eq. 3.2.8.96 represents normal stress difference ratio at the die exit, which is defined as the ratio of the secondary normal stress difference and primary normal stress difference

$$-\frac{N_2}{N_1} = -\frac{\bar{\tau}_{zz}(0) - \bar{\tau}_{yy}(0)}{\bar{\tau}_{xx}(0) - \bar{\tau}_{zz}(0)} \tag{3.2.9.97}$$

note that, in this equation $\bar{\tau}_{xx}(0) - \bar{\tau}_{zz}(0) = 1$ as the result of Eq. 3.2.6.54 and Eq. 3.2.9.89. As it can clearly be seen from Eq. 3.2.8.96, the $-N_2/N_1$ ratio, which characterizes the polymer melt stress state at the die exit region, has to be provided in order to calculate the initial boundary conditions for the extra stress tensor.

Downstream boundary conditions:

Downstream boundary condition, draw ratio, is prescribed as the desired value that is satisfied by a priori unknown magnitude of the drawing force.

$$\bar{u}(X) = DR \tag{3.2.9.98}$$

3.3 Numerical Scheme

To solve the full set of first-order ordinary differential equations, the numerical scheme based on the 4th order Runge-Kutta method implementing adaptive step-size control was adopted. Process of calculation is commenced by guessing a value of drawing force followed by iterative determination of the stress boundary condition at the die through the components of the recoverable elastic strain tensor to satisfy Eqs. 3.2.8.94, 3.2.8.95 and 3.2.8.96 along with the other boundary conditions for the die exit region, that are constant with the force, and thus do not require evaluation in every iteration (Eqs. 3.2.9.89, 3.2.9.90, 3.2.9.91 and $-N_2/N_1$ ratio). Then the main set of eight differential equation is solved in the following order: crystallization kinetics including flow induced crystallization equations (Eq. 3.2.8.82), energy of equation (Eq. 3.2.8.83), film half-width (Eq. 3.2.6.61), axial velocity (Eq. 3.2.7.70), film half-thickness (Eq. 3.2.6.57) and components of the recoverable elastic strain tensor (Eqs. 3.2.7.64–3.2.7.66). Depending on wheatear the desired draw ratio is achieved, the initially estimated drawing force was iteratively updated (increased/decreased) for every following calculation until convergence using the bisection method. Oscillations in the temperature profile development, that were occasionally present in the calculations inflicting the instability of computation, were fixed by applied

stabilizing method of weighting the result of Eq. 3.2.8.83 for actual and previous position *x*. Due to a geometrical symmetry of the film, only $1/4^{th}$ of the film cross-section was used in the calculation as showed in [32]. This basic computational scheme for the determination of unknown process variables was looped according demands of currently conducted parametric studies and eventually complemented by module for a grid linear interpolation to create parametric maps. It was preferred to develop the solver itself in the C++ programming language, to avoid a black box effect, which could have appeared in the case of using a built-in solver in any other commercial mathematical-modeling software. To visualize the obtained data for particular solutions, the solver was coupled with GNUPLOT plotting software for automatic graph generation. Typical computational time for one calculation of prescribed *DR* was about 1 minute on the PC with the following hardware specifications: CPU: Intel Core i7-7700 at 3.60 GHz, RAM: 32 GB DDR4, GPU: AMD Radeon Pro WX 4100 with 4 GB of video memory, SSD: HP Z TurboDrive G2 512 GB. A schematic representation of the utilized numerical scheme is provided in Fig. 6.

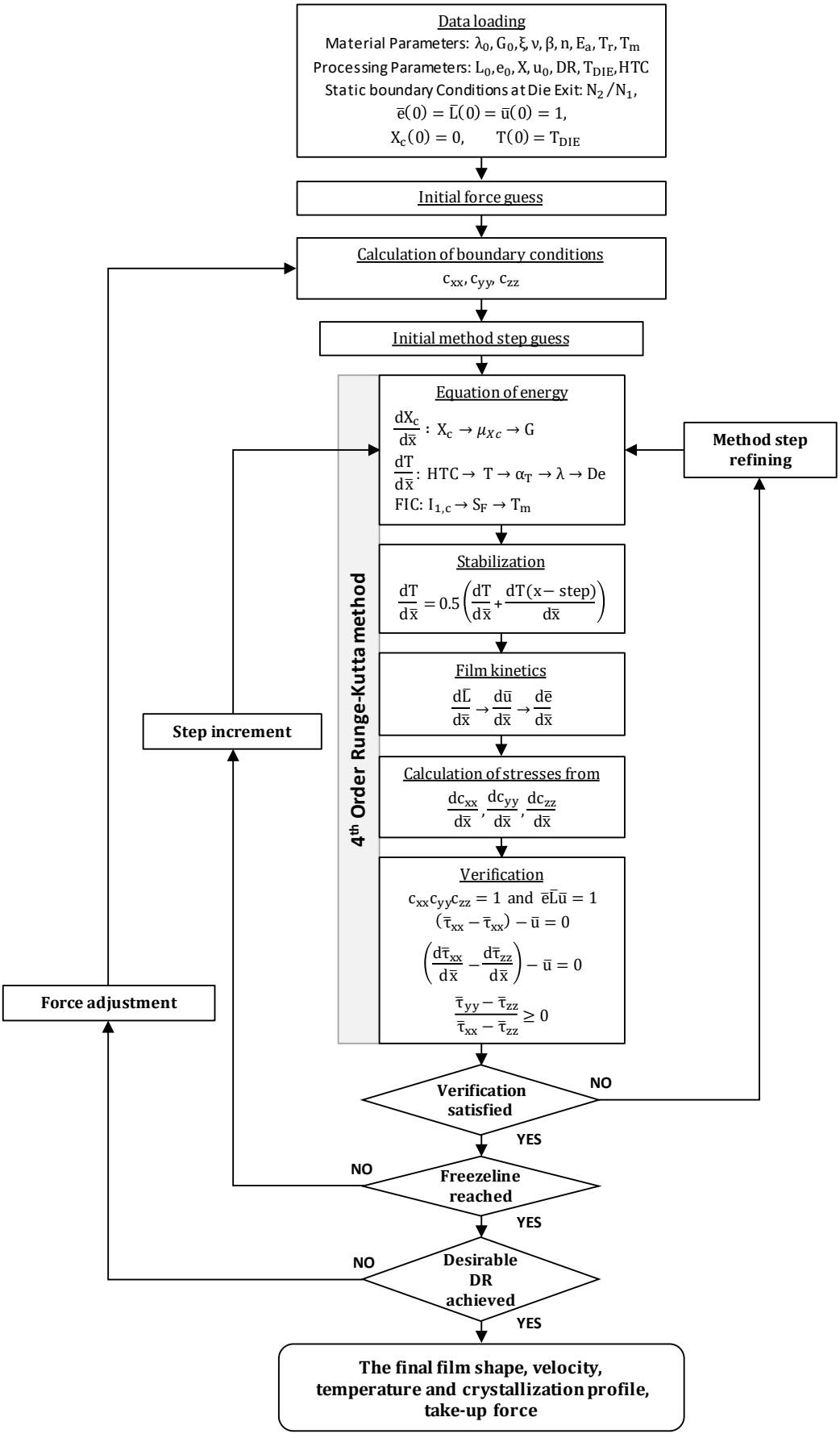

Fig. 6: Flow chart of iteration scheme used to solve of non-isothermal viscoelastic film casting model.

SUMARIZATION OF THE RESEARCH PAPERS

PAPER I–IV

Development of viscoelastic non-isothermal film casting model including temperature and stress induced crystallization

The entire derivation of viscoelastic non-isothermal extrusion film casting model considering temperature and stress induced crystallization is provided in the section 3 of this doctoral thesis.

PAPER I–II

Effect of die exit stress state, Deborah number, uniaxial and planar extensional rheology on the neck-in phenomenon in polymeric flat film production

The effect of second to first normal stress difference ratio at the die exit, $-N_2/N_1$, uniaxial extensional strain hardening, $\eta_{E,U,max}/3\eta_0$, planar-to-uniaxial extensional viscosity ratio, $\eta_{E,P}/\eta_{E,U}$, and Deborah number (via changing the drawing distance, *X*), *De*, on the neck-in, *NI*, has been investigated via viscoelastic non-isothermal modeling utilizing 1.5D membrane model [58] and a single-mode modified Leonov model as the constitutive equation [84, 89]. Based on the performed parametric study, it was found that an increase in $-N_2/N_1$ ratio and *De* increases both, the maximum attainable normalized neck-in, NI^*=NI/X, as well as its sensitivity to $\sqrt{\eta_{E,P}/\eta_{E,U}}$. There exists a threshold value for Deborah number and $\eta_{E,U,max}/3\eta_0$, above which, the NI^* starts to be strongly dependent on the die exit stress state, $-N_2/N_1$. It was found that such critical *De* decreases if $-N_2/N_1$, $\eta_{E,U,max}/3\eta_0$ increases and/or $\frac{\eta_{E,P,max}}{4\eta_0}\Big/\frac{\eta_{E,U,max}}{3\eta_0}$ decreases. Numerical solutions of the 1.5D membrane viscoelastic model, utilizing modified single-mode Leonov model as the constitutive equation, were successfully approximated by a dimensionless analytical equation (Eq. 99) expressing the NI^* with $\eta_{E,U,max}/3\eta_0$, $\eta_{E,P}/\eta_{E,U}$, $-N_2/N_1$ and *De* as follows

$$NI^{*}=\frac{1}{\sqrt[\theta]{\dfrac{\eta_{E,U,max}}{3\eta_0}}}\left\{\begin{array}{l}A_1\left[1-\exp\left(-\alpha_1 De^{\phi_1}\right)\right]\left(\sqrt{\dfrac{\eta_{E,P}}{\eta_{E,U}}}-1\right)+\\ +\delta A_2\left[1-\exp\left(-\alpha_2 De^{\phi_2}\right)\right]\end{array}\right\} \qquad (99)$$

with δ defined as

$$\delta=1+\psi_1\arctan\left(\psi_2\frac{N_2}{N_1}\right)\arctan\left(\psi_3\frac{\eta_{E,U,max}}{3\eta_0}\tanh\left(\psi_4 De\right)\right) \qquad (100)$$

where $A_1=0.593$, $\alpha_1=1073.742$, $\varphi_1=2.113$, $A_2=0.471$, $\alpha_2=99.757$, $\varphi_2=1.162$, $\theta=7.43$, $\psi_1=1.027$, $\psi_2=-0.849$, $\psi_3=0.514$, $\psi_4=3.953$.

Suggested equation was tested by using the experimental data taken from [42], [23, 25, 28] and [7] for five different polyethylenes where $0.011\le De\le 0.253$, $0.825\le\frac{\eta_{E,P}}{\eta_{E,U}}\le 1.910$, $2.047\le\frac{\eta_{E,U,max}}{3\eta_0}\le 10.096$ and $0.017\le-\frac{N_2}{N_1}\le 0.680$. As it can be seen in Fig. 7a, the proposed equation can describe for the given polymer melts and processing conditions the experimental data very well within the whole range of investigated Deborah numbers.

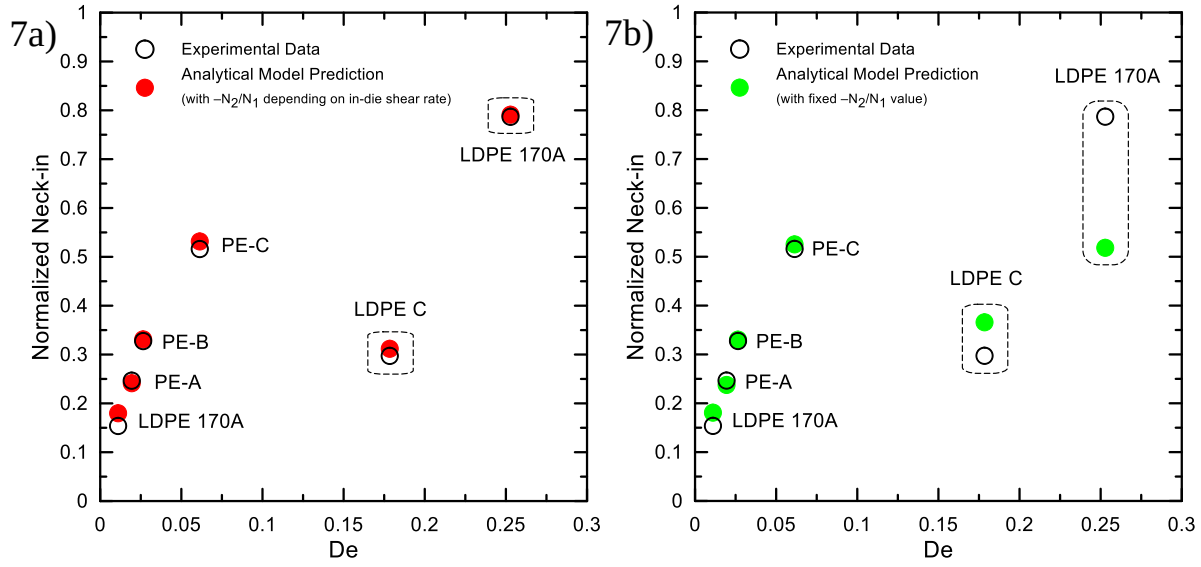

Fig. 7: Normalized maximum attainable neck-in value, NI^{*}, as the function of Deborah number for LDPE 170A, PE-A, PE-B, PE-C, and LDPE C polymers for the processing conditions summarized in Table 6 in [27]. Experimental data (taken from [23, 25, 28], [7] and [42]) and proposed analytical model predictions (Eq. 99) are given here by the open and filled symbols, respectively. (7a) $-N_2/N_1$ is given by the modified Leonov model predictions for particular die exit shear rates, which are provided in Table 7 in [27] for each individual case, (7b) $-N_2/N_1$ is considered to be constant, equal to 0.2.

Interestingly, the neck-in predictions for Deborah numbers larger than 0.1 became unrealistic, if the $-N_2/N_1$ at the die exit region is not taken into account, which confirms the existence of critical Deborah number, above which, the neck-in phenomenon starts to be strongly dependent on the die exit stress state (see Fig. 7b). It is believed that the obtained knowledge together with the suggested simple analytical model can be used for optimization of the extrusion die design (influencing flow history and thus die exit stress state), molecular architecture of polymer melts and processing conditions to suppress neck-in phenomenon in a production of very thin flat films.

PAPER III

Effect of heat transfer coefficient, draw ratio and die exit temperature on the production of flat iPP membranes

In this part, stable numerical scheme has been developed for 1.5D film casting model utilizing viscoelastic modified Leonov model as the constitutive equation [58, 84, 89] and energy equation coupled with crystallization kinetics of semicrystalline polymers taking into account actual film temperature as well as cooling rate [95–97]. Model has been successfully validated on the experimental data for linear isotactic polypropylene taken from the open literature [100].

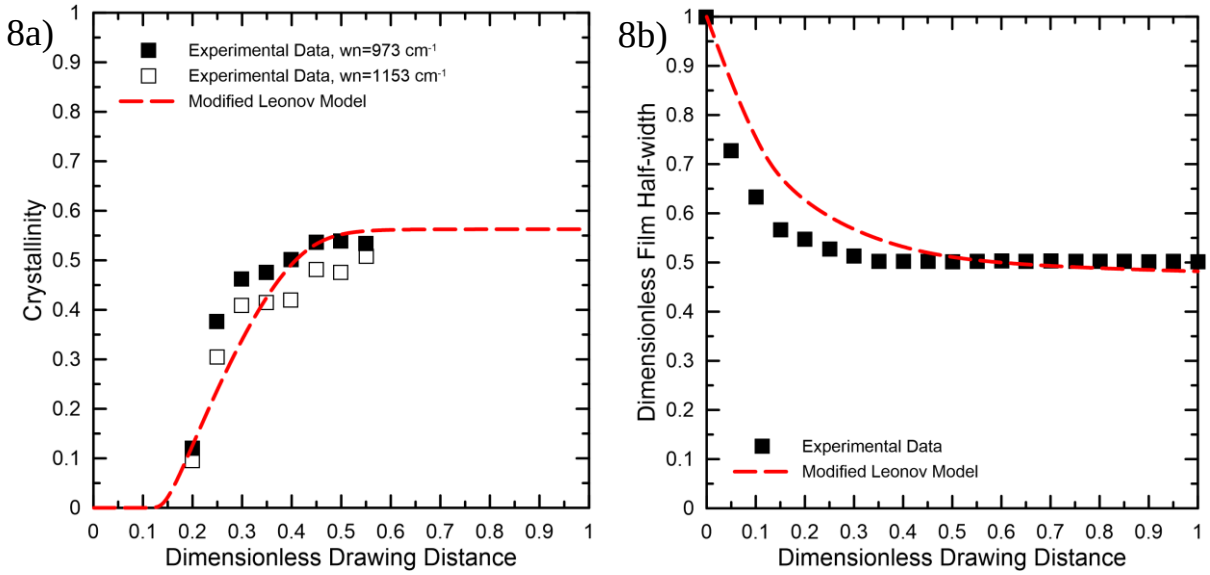

Fig. 8: Comparison between experimental data for iPP T30G (T_{DIE}=200°C) and given processing conditions (De=6·10^{-4}, DR=34.7, X=0.4 m) taken from [100] and model predictions for dimensionless drawing distance variables considering constant heat transfer coefficient, HTC=16 J·s^{-1}·K^{-1}·m^{-2}. (8a) Dimensionless Final Half-width, (8a) Film crystallinity.

Aspect ratio, *A*, (0.25–4), draw ratio, *DR*, (3–140), heat transfer coefficient, *HTC*, (1.5–28 J·s^{-1}·K^{-1}·m^{-2}) and die exit melt temperature, T_{DIE}, (200, 225 and 250°C) were systematically varied in the utilized model in order to understand the role of process conditions on the onset of crystalline phase development in production of iPP flat porous membranes via cast film process. It was found that numerically predicted crystallization onset border in *A* vs. *DR* dependence for given *HTC* and T_{DIE} (see example in Fig. 9a) can be successfully approximated by the following simple analytical equation:

$$A = \exp\left[q_{Xc}(HTC, T_{DIE})\right] DR^{k_{Xc}(HTC, T_{DIE})} \qquad (101)$$

where $q_{Xc}(HTC, T_{DIE})$ and $k_{Xc}(HTC, T_{DIE})$ are given as

$$k_{Xc}(HTC, T_{DIE}) = \left(\gamma_k T_{DIE} + \delta_k\right) HTC^{\left(\alpha_k T_{DIE} + \beta_k\right)} \tag{102}$$

$$q_{Xc}(HTC, T_{DIE}) = \left(\alpha_q T_{DIE} + \beta_q\right) \ln\left(HTC\right) + \left(\gamma_q T_{DIE} + \delta_q\right) \tag{103}$$

These equations utilize 3 independent variables (*DR*, *HTC* and T_{DIE}) and 8 parameters (α_k=−0.0056, β_k=0.3421, γ_k=0.0077, δ_k=−1.2102, α_q=10^{-4}, β_q=−1.0453, γ_q=0.0089, δ_q=−0.3079).

Utilizing isothermal as well as non-isothermal numerical calculations, it was possible to determine processing conditions (in terms of *DR*, *A* and *HTC* at T_{DIE}=200°C) for linear iPP, for which isothermal simulations are too simplistic and therefore the neck-in phenomenon cannot be predicted realistically (see Fig 9b).

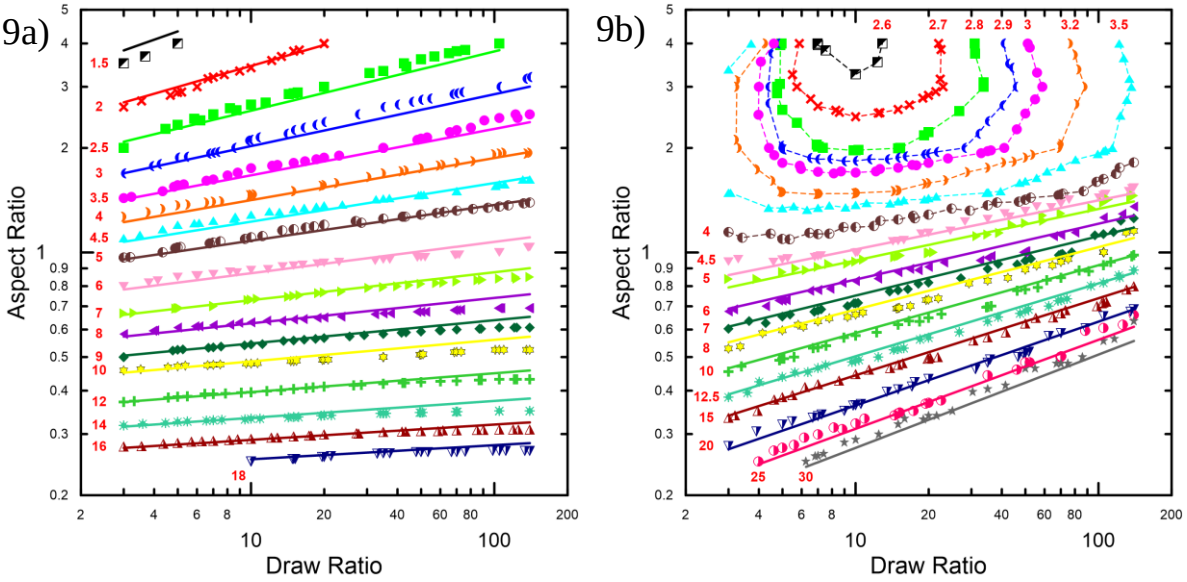

Fig. 9: Effect of draw ratio and heat transfer coefficient (see numbers in $J{\cdot}s^{-1}{\cdot}K^{-1}{\cdot}m^{-2}$ provided at each data set) on the critical aspect ratio for linear iPP at die exit temperature equal to 200°C. (9a) Crystallization onset borders defining conditions for film production with (area above the border symbols) and without (area bellow the border symbols) the crystallized phase, (9b) Isothermality boundaries below which the non-isothermal and isothermal calculations gives practically the same neck-in values.

It was possible to find out the following analytical approximation for the "isothermality boundary" in *A* vs. *DR* dependence for different *HTCs*, which is applicable within the following range of processing variables: $DR \in \langle 3-140 \rangle$, $A \in \langle 0.25-4 \rangle$ and $HTC \in \left(4-30\right\rangle$ $J{\cdot}s^{-1}{\cdot}K^{-1}{\cdot}m^{-2}$.

$$A = \exp\left[q_{iso}(HTC)\right] DR^{k_{iso}(HTC)} \tag{104}$$

where $k_{iso}(HTC)$ and $q_{iso}(HTC)$ are defined as

$$k_{iso}(HTC) = \alpha_{iso} \ln(HTC) + \beta_{iso} \quad (105)$$

$$q_{iso}(HTC) = \gamma_{iso} \ln(HTC) + \delta_{iso} \quad (106)$$

These equations utilize 2 independent variables (*DR*, *HTC*) and 4 parameters obtained by numerical data fitting (α_{iso}=0.067, β_{iso}=0.0406, γ_{iso}=−0.8479, δ_{iso}=−0.9701).

Finally, the effect of *A*, *DR*, *HTC* and T_{DIE} on the dimensionless film half-width and axial velocity, temperature and crystallinity (all as the function of dimensionless drawing distance) was systematically investigated via non-isothermal simulations for linear iPP. It was found that neck-in can be reduced if *A* or *DR* decreases or if *HTC* or T_{DIE} increases. It has also been showed that produced film crystallinity increases if *A* increases or if *DR* or T_{DIE} decreases. The most interestingly, it has been revealed that if the *HTC* increases above some critical value, film crystallinity increases, reaching the maximum and then decreasing. This suggests that there exists optimum *HTC* for given material and processing conditions, at which the amount of crystalline phase is maximal. It is believed that the utilized numerical model together with suggested stable numerical scheme as well as obtained research results can help to understand processing window for production of flat porous membranes from linear iPP considerably.

PAPER IV

Viscoelastic simulation of extrusion film casting for linear iPP including stress induced crystallization

Here, 1.5D film casting membrane model proposed by Silagy [58] was generalized considering single-mode modified Leonov model as the viscoelastic constitutive equation [84, 89], energy equation , constant heat transfer coefficient, advanced crystallization kinetics taking into account the role of temperature, cooling rate [95–97] and molecular stretch [98], crystalline phase dependent modulus [65] and temperature dependent relaxation time [8]. The model has been successfully validated for the linear isotactic polypropylene by using suitable experimental data taken from the open literature as it can be seen in Fig. 10.

It has been found that for the given processing conditions, utilization of flow induced crystallization significantly improves predictions for the film temperature and crystallinity whereas its effect on the neck-in phenomenon and axial velocity profile is predicted to be small. Consequent parametric study has revealed that inclusion of FIC in the model allows to predict realistic plateau in the temperature profile as well as monotonic increase in the film crystallinity for the increased

HTC (see Figure Fig. 10b). It was also shown that there is some threshold HTC value (about 12 $J \cdot s^{-1} \cdot K^{-1} \cdot m^{-2}$ for the studied iPP and given processing conditions), above which melting temperature is changed considerably, abruptly and more closely to the extrusion die due to FIC (see Fig. 11a).

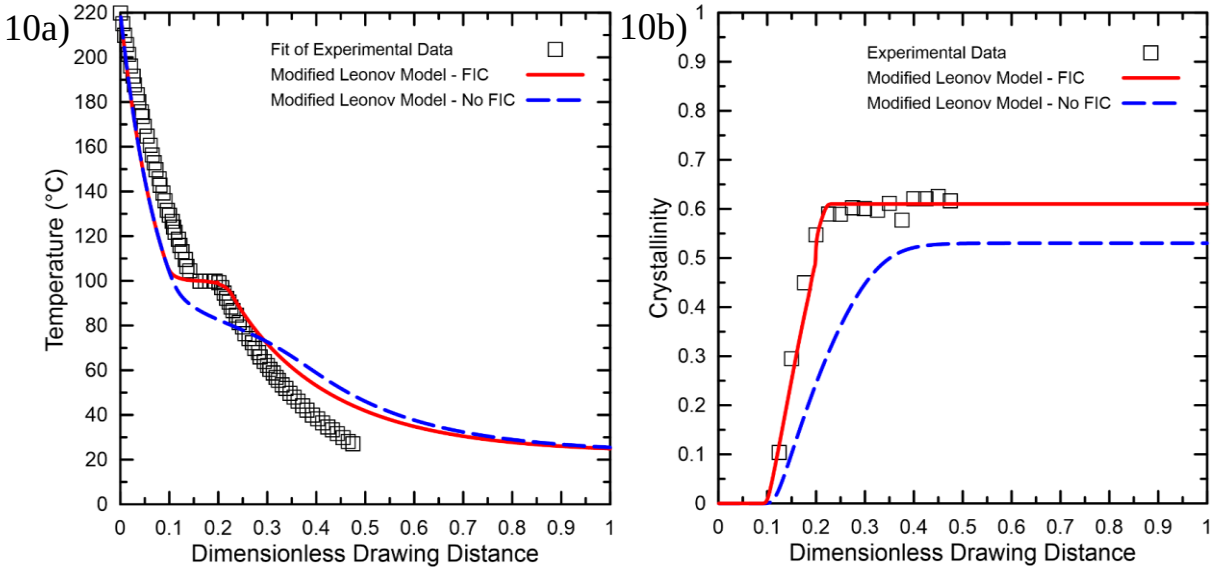

Fig. 10: Comparison between film casting model predictions with and without consideration of Flow Induced Crystallization, FIC, and experimental data taken from [66], HTC=31 $J \cdot s^{-1} \cdot K^{-1} \cdot m^{-2}$. (10a) Temperature profile, (10b) Crystallinity profile.

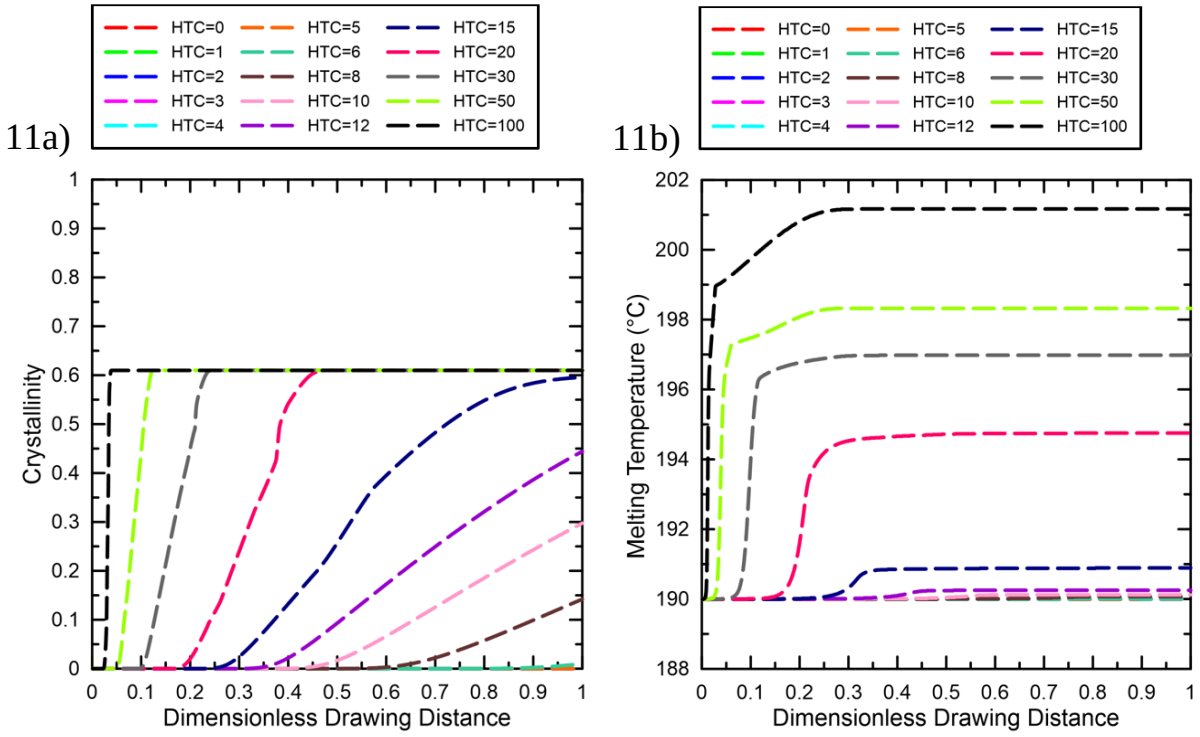

Fig. 11: Predicted effect of HTC on the film crystallinity (left) and melting temperature (right) for iPP at the reference processing conditions.

THE THESIS CONTRIBUTION TO SCIENCE AND PRACTICE

The proposed model and numerical scheme for the viscoelastic, non-isothermal extrusion film casting modeling utilizing a 1.5D membrane model, a modified Leonov model and an advanced crystallization kinetics together with the findings clarifying the fundamental role of variety dimensionless variables (such as planar to uniaxial extensional viscosity ratio, extensional strain hardening, Deborah number, second to first normal stress difference ratio at the die exit, draw ratio, heat transfer coefficient and flow induced crystallization) can be used for material, die design and process conditions optimization in order to minimize unwanted neck-in phenomenon as well as to optimize the extrusion film casting process for different applications of daily and technical use (such as for example separator films for batteries in mobile devices and electric vehicles, foils for capacitors, optical membranes for liquid crystal displays, air and vapor barriers, magnetic tapes for storage of audio video content, packing for consumer products, plastic bags or as product for further processing by other technologies).

The suggested numerical scheme together with the proposed stabilization can be used as the good basic for the viscoelastic non-isothermal modeling of advanced and industrially important polymer processing technologies, in which flow induced crystallization plays the key role.

CONCLUSION

First part of this work summarizes the current state of knowledge in area of polymeric film production via extrusion film casting process and different types of flow instabilities occurring in this technology, such as neck-in, edge beading and draw resonance. Specific attention has been paid to introduction of different approaches for the film casting modeling based on the open research literature.

In the second part of this work, generalized 1.5D film casting membrane model utilizing single-mode modified Leonov model as the viscoelastic constitutive equation and energy equation coupled with advanced crystallization kinetics (taking into account the role of temperature, cooling rate and molecular stretch) has been proposed and successfully tested against relevant experimental data taken from the open literature. By using of the proposed model, it was possible to clarify the role of variety dimensionless variables such as planar to uniaxial extensional viscosity ratio, extensional strain hardening, Deborah number, second to first normal stress difference ratio at the die exit, draw ratio, heat transfer coefficient and flow induced crystallization on the production of polymeric flat films. The key research findings are summarized below:

- It was found that the film casting modeling by using multi-mode XPP model and modified Leonov model is comparable for the given LDPE polymer and processing conditions even if, surprisingly, single-mode version of the Leonov model was used. The consequent parametric study revealed that firstly, if planar to uniaxial extensional viscosity ratio decreases or uniaxial extensional strain hardening increases, intensity of normalized neck-in as well as its sensitivity to draw ratio decreases and secondly, an increase in the second to first normal stress difference ratio at the die exit, $-N_2/N_1$, and Deborah number increases both, the normalized neck-in as well as its sensitivity to planar to uniaxial extensional viscosity ratio. It has also been found that normalized neck-in can be correlated to all the above mentioned variables via a simple dimensionless analytical equation. This correlation can provide detailed view into the complicated relationship between polymer melt rheology, die design, process conditions and undesirable neck-in phenomenon. Obtained results have been validated against literature experimental data for different polyethylene melts and processing conditions.

- It was revealed that there exists critical Deborah number (equal to about 0.1), above which, the neck-in phenomenon starts to be strongly dependent on the die exit stress state, $-N_2/N_1$.

- It was found that numerically predicted crystallization onset border in *A* vs. *DR* dependence for given *HTC* and T_{DIE} can be successfully approximated by the simple analytical equation.

- It was possible to determine processing conditions for linear isotactic PP (expressed numerically or via simple analytical approximation), for which isothermal simulations are too simplistic and therefore the neck-in phenomenon cannot be predicted realistically.

- It was found that normalized neck-in can be reduced if *A* or *DR* decreases or if *HTC* or T_{DIE} increases.

- It has been found that for the processing conditions, in which the cooling rate is very high, utilization of the flow induced crystallization significantly improves predictions for the film temperature and crystallinity whereas its effect on the neck-in phenomenon and axial velocity profile is predicted to be small. Consequent parametric study has revealed that inclusion of flow induced crystallization in the model allows to predict realistic plateau in the temperature profile as well as monotonic increase in the film crystallinity for the increased *HTC*.

- It was shown that there is some threshold *HTC* value, above which the melting temperature is changed considerably, abruptly and more closely to the extrusion die due to flow induced crystallization.

REFERENCES

[1] KANAI, Toshitaka and CAMPBELL, Gregory A. *Film Processing*. Munich : Hanser Publishers, 1999. Progress in polymer processing. ISBN 9781569902523.

[2] KANAI, Toshitaka and CAMPBELL, Gregory A. *Film Processing Advances*. Second Edi. Munich : Hanser Publishers, 2014. ISBN 978-1-56990-529-6.

[3] TADMOR, Zehev and GOGOS, Costas G. *Principles of Polymer Processing, 2nd Edition*. Hoboken, New Jersey : John Wiley & Sons, 2006. SPE technical volume. ISBN 978-0-471-38770-1.

[4] PEARSON, J.R.A. *Mechanics of Polymer Processing*. London : Elsevier Applied Science Publishers, 1985. ISBN 0-85334-308-X.

[5] SMITH, W.S. *Nonisothermal film casting of a viscous fluid*. McMaster University, 1997.

[6] COTTO, D., DUFFO, P. and HAUDIN, J.M. Cast film extrusion of polypropylene films. *Int. Polym. Process.* 1989. Vol. 4, no. 2, p. 103–113.

[7] SHIROMOTO, Seiji, MASUTANI, Yasushi, TSUTSUBUCHI, Masaaki, TOGAWA, Yoshiaki and KAJIWARA, Toshihisa. The effect of viscoelasticity on the extrusion drawing in film-casting process. *Rheologica Acta*. 2010. Vol. 49, no. 7, p. 757–767.

[8] SHIROMOTO, Seiji. The Mechanism of Neck-in Phenomenon in Film Casting Process. *International Polymer Processing*. 2014. Vol. 29, no. 2, p. 197–206.

[9] KOMETANI, H., MATSUMURA, T., SUGA, T. and KANAI, T. Experimental and theoretical analyses of film casting process. *Journal of Polymer Engineering*. 2007. Vol. 27, no. 1, p. 1–28.

[10] DOBROTH, T. and ERWIN, Lewis. Causes of edge beads in cast films. *Polymer Engineering and Science*. 1986. Vol. 26, no. 7, p. 462–467.

[11] BARQ, P., HAUDIN, J.M., AGASSANT, Jean François, ROTH, H. and BOURGIN, P. Instability phenomena in film casting process. *Int. Polym. Proc.* 1990. Vol. 5, no. 4, p. 264–271.

[12] SILAGY, David, DEMAY, Yves and AGASSANT, Jean François. Stationary and stability analysis of the film casting process. *Journal of Non-Newtonian Fluid Mechanics*. 1998. Vol. 79, no. 2–3, p. 563–583.

[13] ZHENG, Hong, YU, Wei, ZHOU, Chixing and ZHANG, Hongbin. Three-Dimensional Simulation of the Non-Isothermal Cast Film Process of Polymer Melts. *Journal of Polymer Research*. 2006. Vol. 13, no. 6, p. 433–440.

[14] ZHENG, Hong, YU, Wei, ZHOU, Chixing and ZHANG, Hongbin. Three dimensional simulation of viscoelastic polymer melts flow in a cast film process. *Fibers and Polymers*. 2007. Vol. 8, no. 1, p. 50–59.

[15] SMITH, Spencer and STOLLE, Dieter. Numerical Simulation of Film Casting Using an Updated Lagrangian Finite Element Algorithm. *Polymer Engineering and Science*. 2003. Vol. 43, no. 5, p. 1105–1122.

[16] BAIRD, Donald G. and COLLIAS, I. Dimitris. Postdie Processing. In : *Polymer Processing: Principles and Design*. Boston : Butterworth-Heinemann, 1995. p. 346. ISBN 9780750691055.

[17] PEARSON, J.R.A. *Mechanical Principles of Polymer Melt Processing*. Pergamon Press, 1966. ISBN 978-0080131504.

[18] BARQ, P., HAUDIN, J.M. and AGASSANT, Jean François. Isothermal and anisothermal models for cast film extrusion. *Int. Polym. Process.* 1992. Vol. 7, no. 4, p. 334–349.

[19] ACIERNO, D., DI MAIO, L. and AMMIRATI, C. C. Film casting of polyethylene terephthalate: Experiments and model comparisons. *Polymer Engineering and Science*. 2000. Vol. 40, no. 1, p. 108–117.

[20] DUFFO, P., MONASSE, B. and HAUDIN, J.M. Cast film extrusion of polypropylene. Thermomechanical and physical aspects. *Journal of Polymer Engineering*. 1991. Vol. 10, no. 1–3, p. 151–229.

[21] LAMBERTI, Gaetano, TITOMANLIO, Giuseppe and BRUCATO, Valerio. Measurement and modelling of the film casting process 1. Width distribution along draw direction. *Chemical Engineering Science*. 2001. Vol. 56, no. 20, p. 5749–5761.

[22] IYENGAR, Vardarajan R. and CO, Albert. Film casting of a modified Giesekus fluid: a steady-state analysis. *Journal of Non-Newtonian Fluid Mechanics*. 1993. Vol. 48, no. 1–2, p. 1–20.

[23] POL, H.V., THETE, Sumeet S., DOSHI, Pankaj and LELE, Ashish K. Necking in extrusion film casting: The role of macromolecular architecture. *Journal of Rheology*. 2013. Vol. 57, no. 2, p. 559–583.

[24] BARQ, P., HAUDIN, J.M., AGASSANT, Jean François and BOURGIN, P. Stationary and dynamic analysis of film casting process. *Int. Polym. Process.* 1994. Vol. 9, no. 4, p. 350–358.

[25] THETE, Sumeet S., DOSHI, P. and POL, H.V. New insights into the use of multi-mode phenomenological constitutive equations to model extrusion film casting process. *Journal of Plastic Film and Sheeting*. 2017. Vol. 33, no. 1, p. 35–71.

[26] BARBORIK, Tomas, ZATLOUKAL, M. and TZOGANAKIS, C. On the role of extensional rheology and Deborah number on the neck-in phenomenon during flat film casting. *International Journal of Heat and Mass Transfer*. 2017. Vol. 111, p. 1296–1313.

[27] BARBORIK, Tomas and ZATLOUKAL, Martin. Effect of die exit stress state, deborah number, uniaxial and planar extensional rheology on the neck-in phenomenon in polymeric flat film production. *Journal of Non-Newtonian Fluid Mechanics*. 2018. Vol. 255, p. 39–56.

[28] POL, H.V., BANIK, Sourya, AZAD, Lal Busher, THETE, Sumeet S., DOSHI, Pankaj and LELE, Ashish. Nonisothermal analysis of extrusion film casting process using molecular constitutive equations. *Rheologica Acta*. 2014. Vol. 53, no. 1, p. 85–101.

[29] CHIKHALIKAR, Kalyani, BANIK, Sourya, AZAD, Lal Busher, JADHAV, Kishor, MAHAJAN, Sunil, AHMAD, Zubair, KULKARNI, Surendra, GUPTA, Surendra, DOSHI, Pankaj, POL, H.V. and LELE, Ashish. Extrusion film casting of long chain branched polypropylene. *Polymer Engineering and Science*. 2015. Vol. 55, no. 9, p. 1977–1987.

[30] POL, H.V. and THETE, S.S. Necking in Extrusion Film Casting: Numerical Predictions of the Maxwell Model and Comparison with Experiments. *Journal of Macromolecular Science, Part B*. 2016. Vol. 55, no. 10, p. 984–1006.

[31] ALAIE, S.M. and PAPANASTASIOU, T.C. Film casting of viscoelastic liquid. *Polymer Engineering and Science*. 1991. Vol. 31, no. 2, p. 67–75.

[32] BEAULNE, M. and MITSOULIS, Evan. Numerical Simulation of the Film Casting Process. *International Polymer Processing*. 1999. Vol. 14, no. 3, p. 261–275.

[33] SHIROMOTO, Seiji, MASUTANI, Yasushi, TSUTSUBUCHI, Masaaki, TOGAWA, Yoshiaki and KAJIWARA, Toshihisa. A neck-in model in extrusion lamination process. *Polymer Engineering and Science*. 2010. Vol. 50, no. 1, p. 22–31.

[34] D'HALEWYU, S., AGASSANT, Jean François and DEMAY, Y. Numerical simulation of the cast film process. *Polymer Engineering and Science*. 1990. Vol. 30, no. 6, p. 335–340.

[35] SMITH, Spencer and STOLLE, Dieter. Nonisothermal two-dimensional film casting of a viscous polymer. *Polymer Engineering and Science*. 2000. Vol. 40, no. 8, p. 1870–1877.

[36] AGASSANT, Jean François, AVENAS, P., SERGENT, J.P. and CARREAU, P.J. *Polymer Processing: Principles and Modeling*. Hanser Gardner Publications, 1991. ISBN 9781569900000.

[37] DEBBAUT, B., MARCHAL, J.M. and CROCHET, M.J. Viscoelastic effects in film casting. CASEY, James and CROCHET, Marcel J. (eds.), *Zeitschrift für angewandte Mathematik und Physik*. 1995. Vol. 46, no. SPEC. ISSUE, p. 679–698.

[38] SHIN, Dong Myeong, LEE, Joo Sung, KIM, Ju Min, JUNG, Hyun Wook and HYUN, Jae Chun. Transient and steady-state solutions of 2D viscoelastic nonisothermal simulation model of film casting process via finite element method. *Journal of Rheology*. 2007. Vol. 51, no. 3, p. 393–407.

[39] RAJAGOPALAN, Dilip. Impact of viscoelasticity on gage variation in film casting. *Journal of Rheology*. 1999. Vol. 43, no. 1, p. 73–83.

[40] KAJIWARA, Toshihisa, YAMAMURA, Masato and ASAHINA, Tomoko. Relationship between Neck-in Phenomena and Rheological Properties in Film Casting. *Nihon Reoroji Gakkaishi*. 2006. Vol. 34, no. 2, p. 97–103.

[41] SOLLOGOUB, C., DEMAY, Y. and AGASSANT, Jean François. Non-isothermal viscoelastic numerical model of the cast-film process. *Journal of Non-Newtonian Fluid Mechanics*. 2006. Vol. 138, no. 2–3, p. 76–86.

[42] SATOH, Naoki, TOMIYAMA, Hideki and KAJIWARA, Toshihisa. Viscoelastic simulation of film casting process for a polymer melt. *Polymer Engineering and Science*. 2001. Vol. 41, no. 9, p. 1564–1579.

[43] AGASSANT, Jean François, DEMAY, Y., SOLLOGOUB, C. and SILAGY, D. Cast film extrusion: An overview of experimental and theoretical approaches. In : *International Polymer Processing*. 2005. p. 136–148.

[44] SAKAKI, Kazutaka, KATSUMOTO, Ryuichi, KAJIWARA, Toshihisa and FUNATSU, Kazumori. Three-dimensional flow simulation of a film-casting process. *Polymer Engineering and Science*. 1996. Vol. 36, no. 13, p. 1821–1831.

[45] GELDER, David. The stability of fiber drawing processes. *Industrial and Engineering Chemistry Fundamentals*. 1971. Vol. 10, no. 3, p. 534–535.

[46] FISHER, Robert J. and DENN, Morton M. Finite-amplitude stability and draw resonance in isothermal melt spinning. *Chemical Engineering Science*. 1975. Vol. 30, no. 9, p. 1129–1134.

[47] FISHER, R.J. and DENN, Morton M. A theory of isothermal melt spinning and draw resonance. *AIChE J.* 1976. Vol. 22, no. 2, p. 236–246.

[48] CHRISTENSEN, R.E. Extrusion coating of polypropylene. *SPE J.* 1962. Vol. 18, p. 751.

[49] MILLER, J.C. Swelling behavior in extrusion. *SPE Trans.* 1963. Vol. 3, no. 2, p. 134–137.

[50] YEOW, Y. Leong. On the stability of extending films: a model for the film casting process. *Journal of Fluid Mechanics*. 1974. Vol. 66, no. 3, p. 613–622.

[51] AIRD, Graham R. and YEOW, Y. Leong. Stability of film casting of power-law liquids. *Industrial and Engineering Chemistry Fundamentals*. 1983. Vol. 22, no. 1, p. 7–10.

[52] ANTURKAR, Nitin R. and CO, Albert. Draw resonance in film casting of viscoelastic fluids: A linear stability analysis. *Journal of Non-Newtonian Fluid Mechanics*. 1988. Vol. 28, no. 3, p. 287–307.

[53] IYENGAR, Vardarajan R. and CO, Albert. Film casting of a modified Giesekus fluid: Stability analysis. *Chemical Engineering Science*. 1996. Vol. 51, no. 9, p. 1417–1430.

[54] SERGENT, J.P. Etude de deux procédés de fabrication de films. Le soufflage de gaine. L'extrusion de film à plat. In : Strasbourg, France, 1977.

[55] TOFT, N. and RIGDAHL, M. Extrusion coating with metallocene-catalysed polyethylenes. *International Polymer Processing*. 2002. Vol. 17, no. 3, p. 244–253.

[56] KOUDA, Shingo. Prediction of processability at extrusion coating for low-density polyethylene. *Polymer Engineering and Science*. 2008. Vol. 48, no. 6, p. 1094–1102.

[57] ITO, Hisahiro, DOI, Masao, ISAKI, Takeharu and TAKEO, Masaaki. A Model of Neck-in Phenomenon in Film Casting Process. *Journal of the Society of Rheology, Japan*. 2003. Vol. 31, no. 3, p. 157–163.

[58] SILAGY, David, DEMAY, Yves and AGASSANT, Jean François. Study of the stability of the film casting process. *Polymer Engineering and Science*. 1996. Vol. 36, no. 21, p. 2614–2625.

[59] NARAYANASWAMY, O.S. A one-dimensional model of stretching float glass. *Journal of the American Ceramic Society*. 1977. Vol. 60, no. 1–2, p. 1–5.

[60] LAMBERTI, Gaetano, TITOMANLIO, Giuseppe and BRUCATO, Valerio. Measurement and modelling of the film casting process 2. Temperature distribution along draw direction. *Chemical Engineering Science*. 2002. Vol. 57, no. 11, p. 1993–1996.

[61] LAMBERTI, Gaetano, DE SANTIS, F., BRUCATO, V. and TITOMANLIO, G. Modeling the interactions between light and crystallizing polymer during fast cooling. *Applied Physics A*. 2004. Vol. 78, no. 6, p. 895–901.

[62] LAMBERTI, Gaetano, BRUCATO, Valerio and TITOMANLIO, Giuseppe. Orientation and crystallinity in film casting of polypropylene. *Journal of Applied Polymer Science*. 2002. Vol. 84, no. 11, p. 1981–1992.

[63] TITOMANLIO, Giuseppe and LAMBERTI, Gaetano. Modeling flow induced crystallization in film casting of polypropylene. *Rheologica Acta*. 2004. Vol. 43, no. 2, p. 146–158.

[64] LAMBERTI, Gaetano and TITOMANLIO, Giuseppe. Analysis of Film Casting Process : Effect of Cooling during the Path in Air. *Industrial & Engineering Chemistry Research*. 2006. Vol. 45, no. 2, p. 719–723.

[65] LAMBERTI, Gaetano and TITOMANLIO, Giuseppe. Analysis of film casting process: The heat transfer phenomena. *Chemical Engineering and Processing: Process Intensification*. 2005. Vol. 44, no. 10, p. 1117–1122.

[66] LAMBERTI, Gaetano. Flow-induced crystallization during isotactic polypropylene film casting. *Polymer Engineering and Science*. 2011. Vol. 51, no. 5, p. 851–861.

[67] ITO, Hisahiro, DOI, Masao, ISAKI, Takeharu, TAKEO, Masaaki and YAGI, Kazuo. 2D Flow Analysis of Film Casting Process. *Journal of the Society of Rheology, Japan*. 2003. Vol. 31, no. 3, p. 149–155.

[68] MCGRADY, C.D., SEAY, C.W. and BAIRD, D.G. Effect of sparse long-chain branching on the film-casting behavior for a series of well-defined HDPEs. *Int. Polym. Process*. 2009. Vol. 24, no. 5, p. 428–438.

[69] SEAY, C.W. and BAIRD, D.G. Sparse Long-chain Branching's Effect on the Film-casting Behavior of PE. *International Polymer Processing*. 2009. Vol. 24, no. 1, p. 41–49.

[70] PIS-LOPEZ, Maria Elena and CO, Albert. Multilayer film casting of modified Giesekus fluids Part 1. Steady-state analysis. *Journal of Non-Newtonian Fluid Mechanics*. 1996. Vol. 66, no. 1, p. 71–93.

[71] PIS-LOPEZ, Maria Elena and CO, Albert. Multilayer film casting of modified Giesekus fluids Part 2. Linear stability analysis. *Journal of Non-Newtonian Fluid Mechanics*. 1996. Vol. 66, no. 1, p. 95–114.

[72] CHRISTODOULOU, Kostas, HATZIKIRIAKOS, Savvas G. and VLASSOPOULOS, Dimitris. Stability analysis of film casting for PET resins using a multimode Phan-Thien-Tanner constitutive equation. *Journal of Plastic Film and Sheeting*. 2000. Vol. 16, no. 4, p. 312–332.

[73] DENN, Morton M., PETRIE, Christopher J.S. and AVENAS, Pierre. Mechanics of Steady Spinning of a Viscoelastic Liquid. *AIChE Journal*. 1975. Vol. 21, no. 4, p. 791–799.

[74] DEMAY, Y. *Instabilité d'étirage et bifurcation de Hopf*. Université de Nice, 1983.

[75] IYENGAR, Vardarajan R. *Film casting of polymer melts*. Orono, ME : University of Maine, 1993.

[76] SMITH, W.S. *Simulating the cast film process using an updated Lagrangian finite element algorithm*. McMaster University, 2001.

[77] DENN, Morton M. *Fibre Spinning*. 1st. Applied Science Publishers Ltd., 1983. ISBN 9789400966345.

[78] BERIS, Antony N. and LIU, Baichen. Time-dependent fiber spinning equations. 1. Analysis of the mathematical behavior. *Journal of Non-Newtonian Fluid Mechanics*. 1988. Vol. 26, no. 3, p. 341–361.

[79] LIU, Baichen and BERIS, Antony N. Time-dependent fiber spinning equations. 2. Analysis of the stability of numerical approximations. *Journal of Non-Newtonian Fluid Mechanics*. 1988. Vol. 26, no. 3, p. 363–394.

[80] DEVEREUX, Brian M. and DENN, Morton M. Frequency response analysis of polymer melt spinning. *Industrial and Engineering Chemistry Research*. 1994. Vol. 33, no. 10, p. 2384–2390.

[81] GAGON, Del Kenneth and DENN, Morton M. Computer simulation of steady polymer melt spinning. *Polymer Engineering and Science*. 1981. Vol. 21, no. 13, p. 844–853.

[82] MINOSHIMA, Wataru and WHITE, James L. Stability of continuous film extrusion processes. *Journal of Polymer Engineering*. 1983. Vol. 2, no. 3, p. 211–226.

[83] LEONOV, A.I. Nonequilibrium thermodynamics and rheology of viscoelastic polymer media. *Rheologica Acta*. 1976. Vol. 15, no. 2, p. 85–98.

[84] LEONOV, A.I., LIPKINA, E.H., PASKHIN, E.D. and PROKUNIN, A.N. Theoretical and experimental investigation of shearing in elastic polymer liquids. *Rheologica Acta*. 1976. Vol. 15, no. 7, p. 411–426.

[85] LEONOV, A.I. and PROKUNIN, A.N. An improved simple version of a nonlinear theory of elasto-viscous polymer media. *Rheologica Acta*. 1980. Vol. 19, no. 4, p. 393–403.

[86] LEONOV, A.I. and PROKUNIN, A.N. On nonlinear effects in the extensional flow of polymeric liquids. *Rheologica Acta*. 1983. Vol. 22, no. 2, p. 137–150.

[87] SIMHAMBHATLA, Murthy and LEONOV, Arkadii I. On the rheological modeling of viscoelastic polymer liquids with stable constitutive equations. *Rheologica Acta*. 1995. Vol. 34, no. 3, p. 259–273.

[88] LEONOV, A.I. Constitutive equations for viscoelastic liquids: Formulation, analysis and comparison with data. *Rheology Series*. 1999. Vol. 8, no. C, p. 519–575.

[89] ZATLOUKAL, Martin. Differential viscoelastic constitutive equations for polymer melts in steady shear and elongational flows. *Journal of Non-Newtonian Fluid Mechanics*. 2003. Vol. 113, no. 2–3, p. 209–227.

[90] RESCH, Katharina, WALLNER, Gernot M, TEICHERT, Christian, MAIER, Günther and GAHLEITNER, Markus. Optical properties of highly transparent polypropylene cast films: Influence of material structure, additives, and processing conditions. *Polymer Engineering & Science*. 2006. Vol. 46, no. 4, p. 520–531.

[91] COPPOLA, Salvatore, BALZANO, Luigi, GIOFFREDI, Emilia, MAFFETTONE, Pier Luca and GRIZZUTI, Nino. Effects of the degree of undercooling on flow induced crystallization in polymer melts. *Polymer*. 2004. Vol. 45, no. 10, p. 3249–3256.

[92] CASTEJÓN, Pilar, HABIBI, Kian, SAFFAR, Amir, AJJI, Abdellah, MARTÍNEZ, Antonio B and ARENCÓN, David. Polypropylene-Based Porous Membranes: Influence of Polymer Composition, Extrusion Draw Ratio and Uniaxial Strain. *Polymers*. 2018. Vol. 10, no. 1, p. 33.

[93] TABATABAEI, Seyed H., CARREAU, Pierre J. and AJJI, Abdellah. Effect of processing on the crystalline orientation, morphology, and mechanical properties of polypropylene cast films and microporous membrane formation. *Polymer*. 2009. Vol. 50, no. 17, p. 4228–4240.

[94] XU, Meng, ZHANG, Shijun, LIANG, Jieying, QUAN, Hui, LIU, Jianye, SHI, Hongwei, GAO, Dali and LIU, Jie. Influences of processing on the phase transition and crystallization of polypropylene cast films. *Journal of Applied Polymer Science*. 2014. Vol. 131, no. 22, p. 41100.

[95] ZIABICKI, A. Crystallization of polymers in variable external conditions. 1. General equations. *Colloid and Polymer Science*. 1996. Vol. 274, no. 3, p. 209–217.

[96] ZIABICKI, A. Crystallization of polymers in variable external conditions. II. Effects of cooling in the absence of stress and orientation. *Colloid and Polymer Science*. 1996. Vol. 274, no. 8, p. 705–716.

[97] LAMBERTI, Gaetano and TITOMANLIO, Giuseppe. Crystallization kinetics of iPP. Model and experiments. *Polymer Bulletin*. 2001. Vol. 46, no. 2–3, p. 231–238.

[98] TITOMANLIO, G., SPERANZA, V. and BRUCATO, V. On the simulation of thermoplastic injection moulding process: II Relevance of interaction between flow and crystallization. *International Polymer Processing*. 1997. Vol. 12, no. 1, p. 45–53.

[99] PANTANI, Roberto, DE SANTIS, Felice, SPERANZA, Vito and TITOMANLIO, Giuseppe. Analysis of flow induced crystallization through molecular stretch. *Polymer*. 2016. Vol. 105, p. 187–194.

[100] LAMBERTI, Gaetano and TITOMANLIO, Giuseppe. Evidences of flow induced crystallization during characterized film casting experiments. *Macromolecular Symposia*. 2002. Vol. 185, no. 1, p. 167–180.

LIST OF FIGURES

Fig. 1: Schematics of the extrusion film casting kinematics. 11

Fig. 2: Visualization of neck-in phenomenon during extrusion film casting. 13

Fig. 3: Visualization of edge-beading phenomenon during extrusion film casting. 14

Fig. 4: Visualization of draw resonance experienced during extrusion film casting. 15

Fig. 5: Visualization of planar and uniaxial extensional flows during extrusion film casting. 18

Fig. 6: Flow chart of iteration scheme used to solve of non-isothermal viscoelastic film casting model. 43

Fig. 7: Normalized maximum attainable neck-in value, NI^{*}, as the function of Deborah number for LDPE 170A, PE-A, PE-B, PE-C, and LDPE C polymers for the processing conditions summarized in Table 6 in [27]. Experimental data (taken from [23, 25, 28], [7] and [42]) and proposed analytical model predictions (Eq. 99) are given here by the open and filled symbols, respectively. (7a) $-N_2/N_1$ is given by the modified Leonov model predictions for particular die exit shear rates, which are provided in Table 7 in [27] for each individual case, (7b) $-N_2/N_1$ is considered to be constant, equal to 0.2. 45

Fig. 8: Comparison between experimental data for iPP T30G (T_{DIE}=200°C) and given processing conditions (De=$6\cdot10^{-4}$, DR=34.7, X=0.4 m) taken from [100] and model predictions for dimensionless drawing distance variables considering constant heat transfer coefficient, HTC=16 $J\cdot s^{-1}\cdot K^{-1}\cdot m^{-2}$. (8a) Dimensionless Final Half-width, (8a) Film crystallinity. 47

Fig. 9: Effect of draw ratio and heat transfer coefficient (see numbers in $J\cdot s^{-1}\cdot K^{-1}\cdot m^{-2}$ provided at each data set) on the critical aspect ratio for linear iPP at die exit temperature equal to 200°C. (9a) Crystallization onset borders defining conditions for film production with (area above the border symbols) and without (area bellow the border symbols) the crystallized phase, (9b) Isothermality boundaries below which the non-isothermal and isothermal calculations gives practically the same neck-in values. 48

Fig. 10: Comparison between film casting model predictions with and without consideration of Flow Induced Crystallization, FIC, and experimental data taken from [66], HTC=31 $J\cdot s^{-1}\cdot K^{-1}\cdot m^{-2}$. (10a) Temperature profile, (10b) Crystallinity profile. 50

Fig. 11: Predicted effect of HTC on the film crystallinity (left) and melting temperature (right) for iPP at the reference processing conditions. 50

LIST OF TABLES

Table 1: Overview of steady-state analyses of film casting process (table adapted from [13–15] and updated for new studies). 17

LIST OF SYMBOLS

Latin Symbols	Meaning	Unit
A	Aspect ratio	1
A_1, A_2	Fitting parameters in analytical model for normalized maximum attainable neck-in	1
A_{ath}	Fitting parameter in crystallization kinetics	1
B_{ath}	Fitting parameter in crystallization kinetics	s
b	Dissipation term	s^{-1}
$\bar{b}$	Dimensionless dissipation term	1
C_p	Specific heat capacity of polymer	$J \cdot kg^{-1} \cdot K^{-1}$
c_{xx}	Normal component of the recoverable Finger tensor in axial x-direction	1
c_{yy}	Normal component of the recoverable Finger tensor in transverse y-direction	1
c_{zz}	Normal component of the recoverable Finger tensor in thickness z-direction	1
$\overset{\circ}{\underline{\underline{c}}}$	Jaumann (corotational) time derivative of the recoverable Finger strain tensor	s^{-1}
$\underline{\underline{c}}$, $\underline{\underline{c}}_{ii}$	Recoverable Finger tensor	1
$\underline{\underline{c}}^{-1}$, $\underline{\underline{c}}_{ii}^{-1}$	Inverse recoverable Finger tensor	1
De	Deborah number	1
DR	Draw ratio	1
$\underline{\underline{D}}$	Deformation rate tensor	s^{-1}
E	Dimensionless take-up/drawing force	1
E_a	Flow activation energy	$J \cdot mol^{-1}$

E_c	Fitting parameter in crystallization kinetics	K
e	Half-thickness of the film at any *x* location	m
e_0	Die half-gap (half-thickness of the film at the die exit)	m
$\bar{e}$	Dimensionless half-thickness of the film at any *x* location	1
$\underline{\underline{e}}_p$	Irreversible rate of strain tensor	s^{-1}
F	Take-up force (drawing force)	N
f	Parameter in function describing the effect of crystallinity on elastic modulus	1
$f(x)$	Rate of deformation in transverse y-direction	s^{-1}
$\bar{f}$	Dimensionless rate of deformation in transverse y-direction	1
G	Linear Hookean elastic modulus (Relaxation modulus)	Pa
G_0	Linear Hookean elastic modulus at the die exit	Pa
$g(x)$	Rate of deformation in thickness z-direction	s^{-1}
$\bar{g}$	Dimensionless rate of deformation in thickness z-direction	1
HTC	Heat transfer coefficient	$J \cdot s^{-1} \cdot K^{-1} \cdot m^{-2}$
h	Parameter in function describing the effect of crystallinity on elastic modulus	1
$I_{1,c}$	First invariant of recoverable Finger tensor	1
$I_{2,c}$	Second invariant of recoverable Finger tensor	1
i	Index *i*, noting the spatial direction	1

j	Relaxation mode identification number	1
$K(t)$	Crystallization kinetics function	s^{-1}
K_{th}	Isothermal function of crystallization kinetics	s^{-1}
k_{iso}	Slope function for determination of isothermal boundary	1
k_{Xc}	Slope function for crystallization on-set	1
L	Half-width of the film at any *x* location	m
L_0	Half-width of the die (half-width of the film at the die exit)	m
$\bar{L}$	Dimensionless half-width of the film at any *x* location	1
MFR, $\dot{m}$	Mass flow rate	$kg \cdot h^{-1}$
m	Parameter in function describing the effect of crystallinity on elastic modulus	1
M_n	Number average molar mass	$g \cdot mol^{-1}$
M_w	Mass average molar mass	$g \cdot mol^{-1}$
NI	Maximum attainable neck-in	m
NI^*	Normalized maximum neck-in value	1
N_1	First normal stress difference	Pa
N_2	Second normal stress difference	Pa
$-N_2/N_1$	Stress state at the die exit	1
n	Non-linear Leonov model parameter	1
n_c	Type of crystallization growth	1
$\underline{n}$	The normal vector to the free surface	1

$P(t)$	Function of non-linear crystallinity evolution	1
p	Isotropic pressure	Pa
Q	Volumetric flow rate	$m^3 \cdot s^{-1}$
q_{iso}	Intercept function for determination of isothermal boundary	1
q_{Xc}	Intercept function for crystallization on-set	1
R	Gas constant	$J \cdot K^{-1} \cdot mol^{-1}$
$\dot{T}$	Rate of cooling	$°C \cdot s^{-1}$
T_{DIE}	Melt temperature at the die	°C
T_m	Melting temperature of polymer	°C
T_{mq}^0	Flow induced equilibrium melting temperature	°C
T	Melt temperature	°C
T_r	Reference temperature in the Arrhenius Law	°C
t	Time coordinate	s
u	Axial velocity component of the film at any *x* location	$m \cdot s^{-1}$
u_0	Axial velocity component at the die exit (velocity in the machine direction)	$m \cdot s^{-1}$
$u(X)$	Chill roll speed	$m \cdot s^{-1}$
$\bar{u}$	Dimensionless axial velocity component of the film at any *x* location	1
$\underline{u}$	The tangential velocity at film-air interface	$m \cdot s^{-1}$
v	Velocity component of the film in transverse y-direction at any *x* location	$m \cdot s^{-1}$

w	Velocity component of the film in thickness z-direction at any *x* location	$m \cdot s^{-1}$
W	Elastic potential	Pa
X	Take-up length (drawing distance, air gap)	m
X_c	Crystallinity content in the polymer volume	1
X_{eq}	Equilibrium level of crystallinity in the polymer volume	1
x, y, z	Spatial coordinates in axial, transverse and thickness direction, respectively	1
x	Position in axial x-direction	m
$\bar{x}$	Dimensionless position in axial x-direction	1
Z	Non-isothermal function of crystallization kinetics	1
Z_x, Z_y, Z_z, X_p	Substitution variables	1
$\frac{dc_{xx}}{d\bar{x}}, \frac{dc_{yy}}{d\bar{x}}, \frac{dc_{zz}}{d\bar{x}}$	Derivative of Finger tensor components with respect to dimensionless $\bar{x}$ position	1
$\frac{d\bar{u}}{d\bar{x}}, \frac{d\bar{L}}{d\bar{x}}, \frac{d\bar{e}}{d\bar{x}}$	Derivative of dimensionless axial velocity, width and thickness with respect to dimensionless $\bar{x}$ position	1
$\frac{dX_c}{d\bar{x}}$	Derivative of crystallinity with respect to dimensionless $\bar{x}$ position	1
$\frac{dT}{d\bar{x}}$	Derivative of temperature with respect to dimensionless $\bar{x}$ position	°C

Greek Symbols	**Meaning**	**Unit**
α_1, α_2	Fitting parameters in analytical model for normalized maximum attainable neck-in	1
α_T	Arrhenius law parameter	1

$\alpha_{iso},\beta_{iso},\gamma_{iso},\delta_{iso}$	Fitting parameters in isothermal boundary function	1
$\alpha_k,\beta_k,\gamma_k,\delta_k,$ $\alpha_q,\beta_q,\gamma_q,\delta_q$	Fitting parameters in crystallization on-set function	1
β	Non-linear Leonov model parameter	1
δ	Shift function in analytical model for normalized maximum attainable neck-in	1
$\underline{\underline{\delta}}$	Unit tensor (Kronecker delta)	1
$\eta_{E,P}$	Steady planar extensional viscosity	Pa·s
$\eta_{E,P,max}$	Maximal steady planar extensional viscosity	Pa·s
$\eta_{E,U}$	Steady uniaxial extensional viscosity	Pa·s
$\eta_{E,U,max}$	Maximal steady uniaxial extensional viscosity	Pa·s
$\frac{\eta_{E,P,max}}{4\eta_0}$	Planar extensional strain hardening	1
$\frac{\eta_{E,U,max}}{3\eta_0}$	Uniaxial extensional strain hardening	1
η_0	Newtonian viscosity	Pa·s
θ	Fitting parameter in analytical model for normalized maximum attainable neck-in	1
κ_1	Fitting parameter in crystallization kinetics	s^{-1}
κ_2	Fitting parameter in crystallization kinetics	1
λ	Melt relaxation time	s
λ_0	Melt relaxation time at the die exit	s

μ_{X_c}	Effect of crystallinity on elastic modulus function	1
ν	Non-linear Leonov model parameter	1
ξ	Non-linear Leonov model parameter	1
ρ_P	Polymer density	$kg \cdot m^{-3}$
σ_{xx}	Total normal stress in the axial direction (machine direction)	Pa
σ_{yy}	Total normal stress in transverse y-direction	Pa
σ_{zz}	Total normal stress in thickness z-direction	Pa
$\underline{\underline{\sigma}}$	Total stress tensor	Pa
τ_{xx}	Normal stress in axial x-direction	Pa
τ_{yy}	Normal stress in transverse y-direction	Pa
τ_{zz}	Normal stress in thickness z-direction	Pa
$\overline{\tau}_{xx}$	Dimensionless normal stress in x-direction	1
$\overline{\tau}_{yy}$	Dimensionless normal stress in y-direction	1
$\overline{\tau}_{zz}$	Dimensionless normal stress in z-direction	1
$\underline{\underline{\tau}}$	Extra stress tensor	Pa
ϕ_1, ϕ_2	Fitting parameters in analytical model for normalized maximum attainable neck-in	1
χ_c	Volume fraction of crystallized phase	1
$\psi_1, \psi_2, \psi_3, \psi_4$	Fitting parameters in analytical model for normalized maximum attainable neck-in	1

LIST OF PUBLICATIONS

Publications in the Journals with AIS abstracted on Web of Science and Scopus Databases

1. BARBORIK, Tomas and ZATLOUKAL, Martin. Effect of die exit stress state, Deborah number, uniaxial and planar extensional rheology on the neck-in phenomenon in polymeric flat film production. *Journal of Non-Newtonian Fluid Mechanics*. 2018. Vol. 255, p. 39–56. AIS=0.769 and IF=2.293 by 2017.

2. BARBORIK, Tomas, ZATLOUKAL, M. and TZOGANAKIS, C. On the role of extensional rheology and Deborah number on the neck-in phenomenon during flat film casting. *International Journal of Heat and Mass Transfer*. 2017. Vol. 111, p. 1296–1313. AIS=0.767 and IF=3.891 by 2017.

3. BARBORIK, Tomas and ZATLOUKAL, Martin. Effect of heat transfer coefficient, draw ratio and die exit temperature on the production of flat iPP membranes. Submitted for publication in: *International Journal of Heat and Mass Transfer*. 2018. AIS=0.767 and IF=3.891 by 2017.

4. BARBORIK, Tomas and ZATLOUKAL, Martin. Viscoelastic simulation of extrusion film casting for linear iPP including stress induced crystallization. Considered for publication in: *Journal of Rheology*. 2018. AIS=1.129 and IF=2.969 by 2017.

Original Full Papers in Conference Proceedings abstracted on Web of Science and/or Scopus Databases

5. BARBORIK, Tomas and ZATLOUKAL, M. Effect of second to first normal stress difference ratio at the die exit on neck-in phenomenon in polymeric flat film production. In: *AIP Conference Proceedings*. Zlin, Czech Republic July 26-27, 2017. 2017. p. 030010. ISBN 978-0-735-41513-3.

6. ZATLOUKAL, Martin, BARBORIK, Tomas and TZOGANAKIS, Costas. On the role of extensional rheology, elasticity and Deborah number on neck-in phenomenon during flat film production. In: *Annual Technical Conference - ANTEC, Conference Proceedings*. Anaheim, California, USA May 8-10, 2017. 2017. p. 1131–1135. ISBN 978-0-692-88309-9.

7. ZATLOUKAL, Martin and BARBORIK, Tomas. Effect of extensional viscosity, elasticity and die exit stress state on neck-in phenomenon during extrusion film casting: Theoretical study. In: *Annual Technical Conference - ANTEC, Conference Proceedings*. Indianapolis, Indiana, USA May 23-25, 2016. 2016. p. 715–719. ISBN 978-0-692-71961-9.

8. BARBORIK, Tomas and ZATLOUKAL, Martin. Effect of viscoelastic stress state at die exit on extrusion film casting process: Theoretical study. In: *AIP Conference Proceedings*. Zlin, Czech Republic July 28-29, 2015. 2015. p. 030013. ISBN 978-0-7354-1306-1.

Conference Contributions not Abstracted in Research Databases

9. ZATLOUKAL, Martin and BARBORIK, Tomas. Effect of Die Exit Stress State, Deborah Number and Extensional Rheology on Neck-in Phenomenon (2018). *Annual Technical Conference - ANTEC*. Orlando, Florida, USA.

10. ZATLOUKAL Martin and Tomas BARBORIK. Effect of die exit stress state, Deborah number, uniaxial and planar extensional rheology on the neck-in phenomenon in polymeric flat film production (2018). *12th Annual European Rheology Conference – AERC 2018*. Sorrento, Italy.

11. ZATLOUKAL Martin and Tomas BARBORIK. Effect of uniaxial and planar extensional viscosities, die exit stress state and Deborah number on neck-in phenomenon during extrusion film casting (2017). *11th Annual European Rheology Conference – AERC 2017*. Copenhagen, Denmark.

12. BARBORIK Tomas and Martin ZATLOUKAL. Effect of Die Exit Stress State, Deborah Number, Extensional Viscosity, Heat Transfer and Crystallization on the Neck-in Phenomenon in Polymeric Flat Film Production (2018). In: *Polymers: Site of Advanced Horizons and Ambits*. Zlin, Czech Republic. ISBN 978-80-7454-729-4.

13. BARBORIK Tomas and Martin ZATLOUKAL. Výzkum jevu Neck-in při výrobě plošných polymerních fólií (2018). In: *Czech Chemical Society Symposium Series 16*. 2018. p. 450. ISSN 2336-7202.

Theses

14. BARBOŘÍK Tomáš. Využití reverzního inženýrství při návrhu vstřikovací formy, *Master Thesis*, Zlin, Tomas Bata University, Faculty of Technology, 2013, p. 116. Supervisor: doc. Ing. Michal Staněk, Ph.D.

15. BARBOŘÍK Tomáš. Konstrukce vstřikovací formy pro plastový díl, *Bachelor Thesis*, Zlin, Tomas Bata University, Faculty of Technology, 2011, p. 69. Supervisor: doc. Ing. Michal Staněk, Ph.D.

CURRICULUM VITAE

Personal Information	
First name / Surname	Tomáš Barbořík, Ing.
Address	Tomas Bata University in Zlín Faculty of Technology, Polymer Centre Vavrečkova 275, 760 01 Zlín Czech Republic
Telephone	+420 57 603 1450
E-mail	tbarborik@gmail.com
Nationality	Czech
Date of birth	7. 4. 1988
Birthplace	Zlín, Czech Republic
Education	
Period	2013–present
Title of qualification awarded	Ph.D.
Principal branch	Technology of Macromolecular Compounds
Organisation providing education	Tomas Bata University in Zlín, Faculty of Technology Polymer Centre
Period	2011–2013
Title of qualification awarded	Ing. (equivalent to M.Sc.)
Principal branch	Process Engineering, Technological Equipment Construction
Organisation providing education	Tomas Bata University in Zlín, Faculty of Technology, Department of Production Engineering

Education

Period	2008–2011
Title of qualification awarded	Bc. (equivalent to B.Sc.)
Principal branch	Process Engineering, Technological Equipment
Organisation providing education	Tomas Bata University in Zlín, Faculty of Technology, Department of Production Engineering
Period	2004–2008
Principal branch	Engineering; specialization: Computer Graphics
Organisation providing education	Secondary Technical School SPS Zlín, Zlín

Research Abroad Stay

Date	2016 (8 months)
Place	Waterloo, Ontario, Canada
Organisation providing training	University of Waterloo, Faculty of Engineering Department of Chemical Engineering

Work on Projects

2016–2018	Grant GA ČR No. 16-05886S *Investigation the effect of polymer melt shear and elongational rheology on production stability of meltblown nanofibers and films* Member of research team
2016	Grant UTB IGA/FT/2016/007 *Modelling of free surface viscoelastic melt flow* Leader of research team

Work on Projects

2015	Grant UTB IGA/FT/2015/013
	Investigation of melt flow stability in flat film
	Leader of research team
2010–2014	Grant GA ČR No. P108/10/1325
	Applied Rheology for Advanced Polymer
	Member of research team

Awards

	Outstanding Master's Thesis Award by the Department of Production Engineering

Conferences

2017	Novel Trends in Rheology VII
2015	Novel Trends in Rheology VI
2013	Novel Trends in Rheology V
	International conferences held by Tomas Bata University
	Member of organization team

Ing. Tomáš Barbořík, Ph.D.

Viscoelastic Modeling of Extrusion Film Casting for Polymer Melts: Investigation of Flow Stability

Viskoelastické modelování extruzního lití polymerních tavenin na válec: Výzkum stability toku

Doctoral Thesis Summary

Published by: Tomas Bata University in Zlín,
nám. T. G. Masaryka 5555, 760 01 Zlín

Edition: published electronically
Typesetting by: Ing. Tomáš Barbořík, Ph.D.
This publication has not undergone any proofreading or editorial review.

Publication year: 2018
First Edition

ISBN 978-80-7454-818-5